DEFINING, ANALYZING AND DETERMINING POWER LOSSES - DUE TO ICING ON WIND TURBINE BLADES

ZANDRA CANOVAS LOTTHAGEN

School of Business, Society and Engineering
Course: Degree Project in Energy Engineering
Course code: ERA403
Credits: 30 hp
Program: Master of Science in Engineering Energy Systems

Supervisor: Jan Sandberg (MDH),
Emil Thalin (Siemens Gamesa Renewable Energy)
Examinor: Konstantinos Kyprianidis
Custumer: Mälardalen Univeristy, MDH
Date: 2020-06-06
Email: zln15001@student.mdh.se

ABSTRACT

The wind power industry is one of the fastest-growing renewable energy industries in the world. Since more energy can be extracted from wind when the density is higher, a lot of the investments made in the wind power industry are made in cold climates. But with cold climates come harsh weather conditions such as icing. The icing on wind power rotor blades causes the aerodynamic properties of the blade to shift and with further ice accretion, the wind power plant can come to a standstill causing a loss of power, until the ice is melted. How big these losses are, depend greatly on site-specific variables such as elevation, temperature, and precipitation. The literature claims these ice-related losses can correspond to 10-35% of the annual expected energy output. Some studies have been made to standardize an ice loss determining method to be used by the industry, yet a standardization of calculating these losses do not exist. It was therefore interesting for this thesis to investigate the different methods that are being used. By using historical Supervisory Control and Data Acquisition (SCADA) data for two different sites located in Sweden, a robust ice determining code was created to identify ice losses. Nearly 32 million data points are being analyzed, and the data itself is provided by Siemens Gamesa which is one of the biggest companies within the wind power industry. A sensitivity analysis was made, and it was shown that a reference dataset reaching from May to September for four years could be used to clearly identify ice losses. To find the ice losses, three different scenarios were tested. The three scenarios use different temperature intervals to find ice losses. For scenario 1 all data points below 0 degrees are investigated. And for scenario 2 and 3 this interval is stretching from 3 degrees and below versus 5 degrees and below. It was found that Scenario 3, was the optimal way to identify the ice losses. Scenario 3 filtered the raw data so that only data points with a temperature below five degrees was used. For the two sites investigated, the annual ice losses were found to lower the annual energy output by 5-10%. Further, the correlation between temperature, precipitation, and ice losses was investigated. It was found that low temperature and high precipitation is strongly correlated to ice losses.

Keywords: Wind Power, De-icing, Defining, Ice losses, Task19, Temperature threshold, Power curve, Big Data.

PREFACE

This thesis is the final work of my Master of Science in Engineering Energy systems at Mälardalen University in Sweden. I want to send many thanks to Siemens Gamesa Renewable Energy for allowing me to conduct this thesis. A special thank you to my supervisor from Siemens Gamesa Renewable Energy, Emil Thalin, for giving me the rare opportunity to get insight into such an extraordinary field and for giving me the trustworthiness to realize his idea. I want to send many thanks to Mikkel Findinge for helping me with the syntax in RStudio and for showing me that no questions are too dumb. At last, thanks to my supervisor Jan Sandberg, for valuable, engaging, and eye-opening discussions.

Västerås in June 2020

Zandra Canovas Lotthagen

CONTENT

LIST OF FIGURES

LIST OF TABLES

DEFINITIONS

Definition	Description
OWI	Software for operating wind turbines with iced blades
Bin	A section of data points which falls within the same interval.

ABBREVIATIONS

Abbreviation	Description
° C	Degrees Celsius
CO_2	Carbon dioxide
IEA	International Energy Agency
IEC	International Electrotechnical Commission
K	Degrees Kelvin
NAN	Not a Number
O&M	Operation & Maintenance
OWI	Operation with Ice
RES	Renewable Energy Source
SCADA	Supervisory Control and Data Acquisition
SMHI	Swedish Meteorological and Hydrological Institute
USD	United States dollar

1 INTRODUCTION

Fossil fuels are being replaced by renewable energy sources (RES) within the next couple of decades; this has made the demand for renewable-powered electricity to grow rapidly. The incentives for the growing demand for RES are founded in climate change action plans from international agreements such as the Paris agreement made in 2015. The consensus of climate change action plans is that global warming exists and that humans are the reason for the carbon dioxide (CO_2) emissions causing this global warming (van der Linden et al., 2015).

The transport sector stands for most of the emissions causing air pollution at ground level from CO_2, which makes primary drivers for the electricity increase. Fossil fueled vehicles need to be replaced, considering electric vehicles are estimated to be over 1 billion in the years to come. Not to mention, the electricity used by industries and residential buildings, this transition has paved the way for RES such as wind and solar power (IRENA, 2019b).

Wind power has been underestimated in numerous energy outlook reports globally throughout the years (Marti, 2017), mainly because no one had foreseen the expansion of wind power made in China (Kåberger, 2020). Despite this, wind power is projected to be one of the world's biggest energy sources in just 30 years: about 86 percent of the power generation is estimated to consist of renewable energy sources, and 50 percent of the final energy consumption - an increase from today's share of 20 percent (IRENA, 2019b). Onshore and offshore wind together are envisioned to stand for more than one-third of the total electricity demand in 2050, and most investments in wind power are made in cold climate countries (IRENA, 2019a). By 2050 the payoff for each United States Dollar (USD) spent on transforming the global energy system will have an outcome of at least 3 USD and provide 7 million jobs worldwide (IRENA, 2019b).

Wind power is created by aerodynamic drag and aerodynamic lift on the wind turbine rotor blades. When the aerodynamic characteristics are changed, it is immediately affecting the power production (Davis, 2014). As of in all energy processes, high efficiency is critical to have a feasible energy production. For wind power, the theoretical maximum efficiency is 59 percent of the energy content of the free wind flow. For manufacturers to assure high energy production to their customers, power losses must be minimized. To do that, the losses need to be identified. Much research is being done on this topic in the wind power industry. The losses can be categorized into aerodynamic energy loss, mechanical loss, and electromechanical losses. Power losses can be further investigated through Supervisory Control and Data Acquisition (SCADA), a system used by manufacturers to trace turbine operational data and other weather-related data. The most common events for a reduction in power generation of wind turbines are down-rating, pitch control malfunction, erosion on wind turbine blades, wind speeds exceeding the boundaries for safe operation, and cold climates: icing on wind rotor blades (Aziz et al., 2019).

1.1 Background

In Sweden, the goal for 2040 is to have a 100 percent renewable energy production for which wind power is expected to stand for the central part of the country's energy mix (IRENA, 2020). As mentioned earlier, most investments in wind power are made in cold climate countries. Wind power is generated by transforming kinetic energy in the wind, which is mostly affected by wind flow since a doubling of it gives eight times the power to mechanical energy in the turbine. Cold climates generally have a higher wind velocity and higher air density, which results in higher kinetic energy (Stoyanov et al., 2020).

Be that as it may, there are some problems in colder climates in the form of icing on rotor blades, which can cause big power losses. Ice accretion increases aerodynamic drag and decreases aerodynamic lift (Davis, 2014). The most frequent problems caused by ice losses are reduction of aerodynamic efficiency due to characteristic change in blade aerodynamics, turbine loads, components lifetime, increase in the noise created by blades, safety hazards, and measurement errors. The annual production losses due to icing are relatively high and can stand for 10 % up to 35 %, according to Hansson et al., (2016) and Yirtici et al., (2019). Therefore, many wind turbines are installed with a de-icing system and other systems that are used to overhaul the losses as fast as they occur.

It is challenging to identify when ice losses occur compared to identifying other events, and there is no standardized way of determining when the icing is affecting power production and cause depletion (Davis, 2014). The methods used today are general and miss several essential factors. The International energy agency (IEA) started Task 19, "Wind energy in Cold Climates" in 2002, which later developed the "Task 19 Ice Loss Method" which is a method for determining ice losses (Laakso et al., 2009). Another method for determining ice-losses is the Kjeller method created by the consulting firm Kjeller Vindteknikk. Both methods are used widely in the industry.

1.2 Aim

In this report, the first issue is to define ice-losses and to examine further when they occur. This will be done by developing a code that can calculate power production losses due to direct icing on rotor blades by analyzing historical SCADA data from wind farms. The result should be able to be used as a solid model to identify when ice losses occur and why to demonstrate the importance of de-icing systems. The aim is to investigate further whether the geographical location and other factors such as temperature or precipitation have any correlation with the ice losses.

1.3 Research questions

- How are energy losses due to icing defined in terms of temperature thresholds and power curve degradation?
- Can ice-losses be identified by analyzing SCADA data?
- Can a model be developed to determine the power losses due to icing?
- How substantial are the energy losses due to direct ice formation on rotor blades of a wind power plant?
- Do factors such as temperature and/or precipitation have any correlation with ice losses?

1.4 Delimitation

To tailor this report in the size of a master's thesis, the work has been delimited, and the following points will not be considered:

- The production of energy in the technical aspects will be evaluated yet the economic aspects of lost energy production will not be considered in the report.
- Factors like noise and ice throw are not evaluated.
- Wear and tear on materials and mechanical parts are not within the scope of this thesis.
- This model can only be used for SCADA data from pitch-regulated turbines, which is the most common turbine type in the industry today.

2 METHODOLOGY

Initially, a literature study is made to gather information and evaluate the methods that are used today to determine ice-losses to assess the right approach for this thesis. As mentioned in the Introduction section, there are two significant methods of determining ice-losses that are used today: The Kjeller method and the IEA Task 19. The literature study should also consist of different types of approaches to clean data for not a number (NAN) type of values and inaccurate data such as outliers which can affect the end result. Further, some frequently used terms are clarified under section 2.3 to avoid any misunderstandings.

2.1 Literature review

Different library databases such as Primo are used to search for relevant studies. Google scholar is also being used as the main gateway. The search is mainly filtered to 2016-2020 to get the latest discoveries in this fast-growing wind industry, but due to a narrow research field, the author has been forced to go beyond this time span. Some literature has also been gathered from the University library. The foundation of the analysis is based on SCADA data received from the partnership company, Siemens Gamesa Renewable Energy, which is one of the largest companies within the wind power business (Reuters, 2016) and will in this report be referred to as SGRE. The site location will, however, not be mentioned in this report, and the site names will be anonymized, identified as Site 1 and Site 2. The ice losses will be normalized with a manipulation factor, and the results will be normalized to the percentage of the rated power of the turbine - a precaution to delimit the risk of exposing confidential information in a competitive industry.

SCADA data or Supervisory Control and Data Acquisition is an industrial control system that is used in the wind power industry to monitor, gather, and process real-time data. The data is typically stored in a 10-minute resolution with records for numerous parameters for every turbine 365 days/year. There are four major categories of data variables: environmental parameters (e.g., wind speed, wind direction, ambient temperature); electrical parameters (e.g., active power); component temperatures (e.g., gearbox bearings temperature) and control variables (e.g., pitch angle, rotor speeds). Other information gained from SCADA is status codes and alarms. (Aziz et al., 2019)

2.2 Data collecting and handling

Information about the wind power industry in general, but also recognition of problems regarding icing, and possible solutions to these will be received from the attendance at the Winter Wind conference held in Åre, Sweden. Winter Wind is the biggest conference in the world that treats wind power in cold climates. Each year scientists, engineers, manufacturers, developers, consultants, investors, wind farm owners, and Operation & Maintenance (O&M) providers, as well as representatives from government agencies from all over the world, gather in Sweden to discuss the challenges of generating wind power in cold climates.

The data given by SGRE will be normalized in this thesis, and site names will be modified due to the confidentiality and rivalry agreement made within SGRE. To begin with, SCADA data will be investigated for one month at a time for one site. A method for cleaning of data will then be selected, and that is when the data can be analyzed. When the model has been validated with sensitivity analyses, and the results have been confirmed by the findings of other similar reports, the model should be able to be extended to other wind power parks within SGRE and in a prolonged time resolution of several years. The resulting power losses are manipulated with a factor. These manipulated figures should give insight into the difference between the calculated ice losses without releasing any official figures of the power losses.

This means that the software for which the model is to be calculated must handle big data. Because of this, the software RStudio, which operates with the program language R, which is chosen since it is a language for statistical computing and graphics. RStudio can also handle big numbers of data points easy and is open access, which makes it very applicable in this type of investigation.

2.3 Further clarifications

Operation with ice (OWI) is the name of the software used by Siemens Gamesa. The same type of software is used by many manufacturers but goes under other names. The software is further explained in section 3.4 but will be referred to as OWI.

Bin is a common term in the wind power industry used to describe an interval. More thoroughly, it is a term for describing a section of data points with multiple wind speeds that fall within the same range. The range can vary, but, commonly, a range covers 0.5 m/s per bin. The concept of binning was established to get smooth power curves.

3 LITERATURE STUDY

Yirtici et al. made a report in 2019, where they investigated a methodology to evaluate ice-induced power losses on horizontal axis wind turbines by predictions of ice formations and investigated different types of ice formations. According to Yirtici et al. (2019), it is well-known that icing occurs when supercooled droplets in the atmosphere access a surface such as a turbine blade. Droplets may either freeze instantly and form rime ice on the surface or may run downstream and freeze to later form a glazed ice structure. The blades have the crucial task of capturing the wind flow. Icing affects the aerodynamic performance of the rotor blades by lowering the lift force, which increases the drag force. Aerodynamic disruption can lead to a complete stoppage of the turbine, which can end with a full power loss.

There is a high interest in optimizing the wind power industry. Numerous studies have been made to model safe forecast methods for wind power production. Pinpointing when production losses due to icing are happening is difficult: yet not impossible. Several studies (Byrkjedal et al., 2015; Gonzalez et al., 2019; Homola et al., 2009; Skrimpas et al., 2016; L. Zhang et al., 2018) have managed to identify power losses due to icing. However, it is important to emphasize that the number of methods that exist to identify ice losses is equal to the number of studies, which makes the variance in methods used very high.

In the literature, studies with sensitivity analyses are, in general, absent. Mainly since the primary aim in most studies is the reduction in prediction error of the forecasting or they have other agendas. Rather than to solely identify icing losses. This makes a gap in the literature, a gap which the author of this report is hopeful to be able to fill by this literature study.

3.1 Pitch regulated turbines

The power output controlled by the velocity at a predetermined level is called power regulation. This predetermined level can vary between manufacturers but is usually set to between 12 and 16 m/s. It can also be set to an appropriate level based on the wind conditions at the site, or the ratio between the rotor length and the generators rated power (Sathyajith, 2006). Wind power turbines have their maximum aerodynamic performance at a given angle of attack. The angle of attack of a blade profile changes with the wind velocity and the rotor speed. In a pitch-controlled wind turbine, there are electronic sensors that continuously monitor the variations in power produced by the system. The output power is checked several times in a second. With the variations in power output, the pitch control mechanisms are activated to adjust the blade into a desirable angle. When the wind reaches rated speed, the blades are turned, so the power does not exceed the rated power (Wizelius, 2015).

3.2 Power curve

In “Handbook for wind energy engineering” from (2017), Letcher explains the characteristic power curve for a pitch regulated turbine. Letcher defines the minimum speed for which electricity can be generated as cut-in speed. All wind speeds below a threshold, which is typically around 4 m/s, does not generate enough rotational power to kick-start the turbine. This is illustrated in Region 1 in Figure 1. Region 2 in Figure 1 shows how the power generated is increasing with higher wind speeds which is then regulated in Region 3 when the rated power is obtained. The rated power is defined by the maximum rotational speed limit for which the rotor is allowed to run. This speed limit is often set by the manufacturer to increase the longevity of the blades by preventing and minimizing bird impacts, rain and erosion according to Letcher. At the cut-off wind speed at typically 25 m/s, which is also the maximum wind speed, the rotor is brought to a standstill by a break to prevent structural damages. The wind speeds over 25 m/s generate power but are regulated to not exceed the 25m/s threshold for safety reasons by pitching the blades.

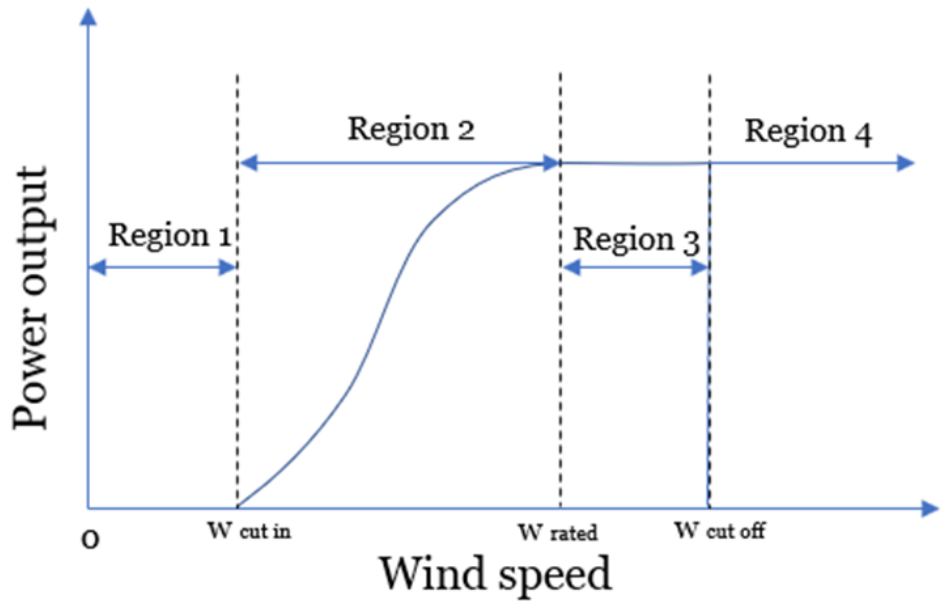

Figure 1 - A characteristic power curve for a pitch regulated wind turbine, Inspired by Sohoni et al. (2016).

Power curves are an easy way to illustrate the relationship between the output power and wind speed. A typical power curve for a pitch regulated wind turbine has a cut-in speed and a cut-out speed. In Figure 1, inspired by Sohoni et al. (2016), a power curve is shown, which is typical for a pitch regulated wind turbine.

3.2.1 *Issues with Power Curve Modelling*

Many attempts have been made to identify periods of nominal and fault operations of wind turbines with the help of power curves, and some have further tried to calculate production losses and tried to identify them. The methods vary a lot, but the most used way is to look at power curves. Power curves can be helpful when checking the performance of a turbine. It can be used for forecasting production or, if data is at hand, to calculate power losses. As earlier mentioned, different assumptions are made when trying to identify icing, and there is no standardization, which makes the results very variant. A few minor deviations in assumptions and limitations can cause considerable alterations in the final result, causing disparity site-wise giving questionable results.

In 2016 Vaishali Sohoni, S.C. Gupta and R. K. Nema wrote in their critical review on modeling wind turbine power curves that there are several essential issues to consider while modeling a power curve. They stated five main issues; Difference in turbine models, Cut-in and Cut-off behavior, Single versus a group of turbines, Influencing factors, and International Electrotechnical Commission (IEC) 61400-12-1 Standard. Four issues being of enough relevance to get a further explanation in the titles that follow.

3.2.1.1. Difference in turbine models & Cut-in/Cut-off

Power curves will differ depending on manufacturers and models. The characteristics will then be different depending on the cut-in and cut-off behavior of the turbine. There are two main ways of handling turbines near cut-in and cut-off wind speeds; Pitch regulation and stall regulation. Stall regulated turbines have solid rotor blades, whereas pitch-regulated wind turbines which are dominating the market today can pitch the rotor blades.

The cut-off and cut-in fluctuation behavior that occurs between shut down and restart of the turbine affects the productivity of the turbine. The effect has on the productivity change depending on wind patterns and terrains referred to as hysteresis in the literature, where turbulent winds require more frequent starting and stopping.

3.2.1.2. Single turbine versus Wind farm

A prediction of the power output is always given by the manufacturer; this prediction is presented in a power curve for the specific turbine type at hand. Wind energy production is highly affected by the stochastic nature of the wind. In a wind farm, one turbine can have a different power output from a nearby turbine of the same turbine model. This can be caused by shadowing effects, also called wakes. A single wind turbine causes the downstream wind (the wind behind the plant), which disturbs the upstream wind flow for a nearby plant. The difference can also lay in wear/tear, aging, dirt, or ice deposition on blades. Sohoni et al. stress the importance of considering this while modeling big wind power farms.

3.2.1.3. Correlation factors

Correlation factors or influencing factors, as one might call them, are factors that cause the power curve to depart from the theoretical value. By taking various site-specific factors into account, it can be easier to understand the resulting power curve. The wind is the prime factor that affects the power output, and therefore the power curve. Trees, buildings, and other topologies at site influence the direction and velocity of wind streams. Blade geometry, which is disturbed when there is ice build-up on blades, leaves the aerodynamics of the blade alteration, which causes power output deterioration.

Air density is changed due to pressure, temperature, and humidity on site. And is directly correlated to ice accretion and, therefore, power production. By normalizing data from air density just like St. Martin et al.,(2016) did in their report, it is much more likely that outliers from other influencing parameters will be found and that the power production losses are better reflecting the reality. The vibration of the nacelle and tower is also a factor caused by ice accretion. In 2016, Skrimpas et al., a study where they detected ice build-up by utilizing a power curve and nacelle vibration data.

Temperature is a critical factor for ice accretion; water freezes as the temperature go below 0 degrees Celsius. Depending on the temperature, different types of ice formations are created. There are typically two types of icing conditions stalked about in the wind industry: metrological icing and instrumental icing. Metrological icing occurs when the metrological conditions for ice accretion are favorable. Rime ice forms at temperature from 0° C down to -40° C. Glaze ice, however, is usually formed at a combination of high speeds, high temperatures (between 0° C and -6° C), and high liquid water content (Yirtici et al., 2019). Instrumental icing is periods when ice remains at a structure and/or an instrument. Logically, ice does not disappear at the same time as the temperature goes above 0° C.

3.2.2 *SCADA data*

What Sohoni et al. fails to mention it their report from 2016, is the fact that wind speed measurements on a turbine are made by an anemometer that is placed in the back of the rotor. This means that the anemometer is placed in the wake of the rotor leading to big uncertainties regarding the actual wind velocities. Laakso et al., (2010) claim in their study that the wind speed underestimations can be as high as 30%. Manufacturers are using a correction factor in SCADA to improve the accuracy of the data, yet there is still a big uncertainty with the measurements.

In the studies where SCADA data have been available, the structure for identifying icing losses follows the same structure which is illustrated in Figure 2. The input data or the SCADA is used to make a reference power curve that should reflect the ideal power production of a turbine and/or an entire site. A reference power curve is a curve for the optimal performance of a turbine or can be made to represent an entire wind farm. SCADA provides alarm codes which are normally indicating that the turbine is operating in normal condition versus when it is not. A classification of when icing is supposedly happening is done and the data is then filtered based on classifications of icing events. The production losses are then calculated by identifying the ice-losses which is done by comparing the reference curve with the data points classified as icing events.

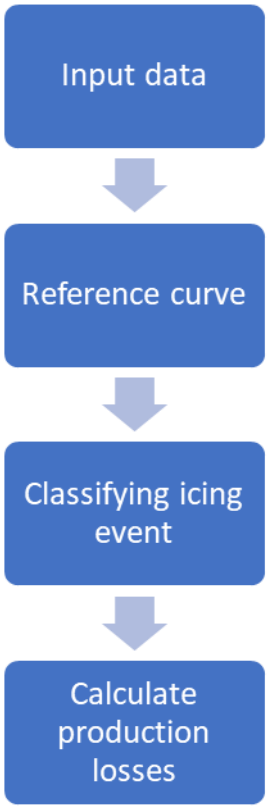

Figure 2 - Typical process scheme over ice-loss identification of SCADA data with a Power curve approach.

3.3 Methodology Approaches

Hansson et al. (2016) wrote a report on quantification of icing losses in wind farms as a part of Energiforsk's research program Vindforsk IV which was carried out by Kjeller Vindteknikk. In the report, three main ways of defining ice-losses were found and further explained. The first method presented; estimated ice losses based on a comparison between summer and winter power curves. Turbulence, atmospheric stability, and air density may be substantially different during winter as compared to summer which is an issue that Energiforsk highlight in their report. This would inadequately represent the expected power during winter with the power curve estimated based on summer data.

The second method, based on analyzing the variations around the power curve and assuming these variations will equal out if analyzed over a long enough time. Possible deviations from this would then be caused by icing. Energiforsk means that this method can give reasonable estimations of icing long-term but when shorter periods are investigated the method fails to estimate icing losses.

Lastly, a method of putting a threshold value on the power curve and identify periods when the power production comes below these threshold values as periods with icing is presented. The power tends to fluctuate around a given power curve depending on other parameters such as wind direction, atmospheric stability, and turbulence. Energiforsk points out that the method might not be able to find all the cases for which icing losses occur, but might, on the other hand, identify periods that can be associated with icing although icing is not the problem.

3.3.1 *Classification of icing losses*

Research by Aziz et al. (2019) amongst others (Byrkjedal et al., 2015; Davis et al., 2015; Hansson et al., 2016; Sohoni et al., 2016) have used SCADA data to create prediction models and/or models for measuring icing losses. SCADA covers all the data needed to perform power curves. Depending on the data needed at hand, a dataset from SCADA can cover millions of data points which makes it a powerful source of knowledge. There are however different assumptions made while making power curves. Byrkjedal et al., use the same method as Davis et al., where SCADA data is used to calculate the power curve by taking the median power values from wind speeds binned with 0.5 m/s intervals, an IEC standard according to Sohoni et al. (2016).

In the report by Byrkjedal et al. from 2015, an operational forecasting model for icing is developed for four wind farms located in Sweden. Data from 12 Swedish metrological stations are used to develop the model. The reference data that is used for the model calculates the power curve by using SCADA data. The report is therefore interesting to look at since the reference data use the median power output values from all wind power sites, and divide, or bin, them into 0.5 m/s intervals. Data for periods with curtailed power output is removed, they are also looking at alarm codes. An alarm code is removed along with the data from the pro- and preceding 10-minute time steps. The data is further analyzed by filtering all data points which have a temperature below 3 °C if these fall below the 10th percentile threshold of the median power for more than 3 consecutive time steps or 30-minutes they are classified as icing. Even though the main purpose of the study was to forecast icing, the resulting ice-losses identified from the SCADA data are highly interesting to look at. The ice-losses for the sites were observed to be 22%, 9%, 10%, and 13% respectively for each site. Justification as to why the results diverge is yet to be given.

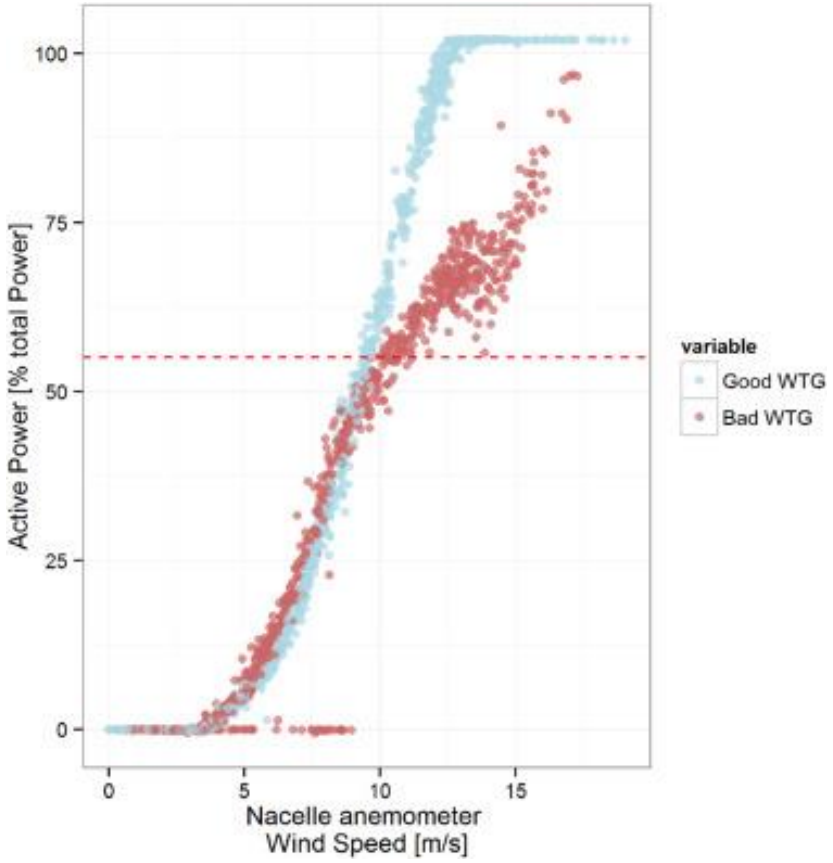

Figure 3 - Normal vs abnormal power curve. Retrieved from: Papatheou et al. (2017).

The approach for data cleaning made by Byrkjedal et al. (2015b) was to first remove data points when the turbine was identified to be in a derated state. Thereafter, data points with error codes that could not be linked to icing were removed. The data point before and after the error code was also removed since the error flags were only given to the classic 10-minute interval given by SCADA. The only indications for icing were therefore the data points following each other of a minimum of 3 consecutive time steps. Byrkjedal stated that the

uncertainty with this method is that there is no way to know exactly when the error occurred due to the 10-minute time step of the SCADA data.

In a report by Davis et al. (2015) four wind parks with known icing occurrences were investigated and compared with each other. Three different methods were used to observe indirect ice detection using a power curve deviation. Davis et al. (2015) concluded that setting an ice threshold of the 10^{th} percentile of the observed power curve data during normal operation with a 2-h minimum duration was the best approach for identifying ice-losses. The reference power curve was based on 40 % of the total percentile to fit the local regressions since the raw data made the percentile curves quite ragged due to outliers. The suggestion is to base the percentile on data for at least one year. Further, a smoothing function was suggested to be applied to the percentile to remove outliers which would be caused by limited numbers of data points. A positive 2.5° C bias in the nacelle temperature was also found in one of the two turbines that were studied. They also investigated different scenarios where the temperature threshold for iced data was set from -2° C to +4° C.

Homola et al. wrote a report in 2009 about energy production losses due to iced blades and instruments for three wind power sites in Norway and Sweden. They use power curves to identify ice losses with both 10-minute and 1-hour historical data, it is however not specified if the data is SCADA data. Since the expected power curve is based on data of the median power production between the 1st of May to 1st of October where data points with an ambient temperature above +2° C were used, it is safe to imply that the data in hand is indeed given by SCADA. They divide the wind speeds into 0.5 m/s bins, just as (Byrkjedal et al., 2015; Davis et al., 2015). Wind speeds lower than 5 m/s were filtered out due to the nonlinearities associated with starting and stopping the turbine. An 85% threshold was set to identify low power production due to ice. The difference between the expected power from the power curve and the actual power was counted as a power loss.

In comparison to the other studies mentioned, Homola et al. (2009) use a reference power curve that uses both non-iced data and iced data. The method is, therefore, underestimating the power losses since the power curve is based on all data to generate the power curve. Some problems with overproduction which were linked to the anemometers were also identified. The anemometers were giving a too low value which thereby gave an unrealistic good power production. However, the calculated losses were only 0.5 percent for this site with Siemens turbines which in contrast to the other two sites is very low, mainly due to the faulty values from the anemometer. The threshold was therefore modified to 115 percent of expected power plus 50kW for velocities over 3 m/s. The second site had a production loss of 5 percent whereas the third site had more than four times higher production losses during winter compared to summer, both being Vestas turbines. For the third turbine that means that the average production losses where 27.9% during winter compared to 6.6% during summertime.

3.3.2 *Task 19*

Though it might seem like there is no standardized way of detecting ice-losses, IEA founded a task group in 2002 called: Task group 19 – a division in IEA founded to gather and provide information about wind energy in cold climates. In 2019, Task 19 published a method for determining production losses. The method, called task 19 IceLoss method (2019), use SCADA data to calculate icing losses and is publicly available as a Python code released on GitHub in 2019. The method is acknowledged by the industry, yet due to its recently being published, there are no studies made to validate the method.

The method complies with Energiforsk's findings of three types of methods. However, Task 19 IceLoss method combines the three methods mentioned by Energiforsk in a new way which deals with the main issues also stated by Energiforsk. Task 19 further affirm a warning about nacelle temperatures which in some cases have shown a constant bias of +2 to 3°C due to radiation heat of the nacelle. Task 19 also states that ice build-up deteriorates the power output or results in overproduction due to iced anemometers.

3.3.2.1. Reference Power Curve

The structure of the method is based on percentiles of the reference power curve which is created by non-iced data classified by data points above an ambient temperature of 3° C. Air density is corrected to hub height and since air pressure is normally not given by SCADA data, static pressure is calculated based on on-site elevation above sea level. Site air density and pressure are then used to calibrate nacelle wind speeds as follows:

Equation 1

$$w_{site} = w_{std} * \left(\frac{\rho_{std}}{\rho_{site}}\right)^{\frac{1}{3}} = w_{std} * \left(\frac{\frac{P_{std}}{T_{std}}}{\frac{P_{site}}{T_{site}}}\right)^{\frac{1}{3}}$$

Equation 2

$$w_{site} = w_{std} * \left(\frac{T_{std}}{T_{site}}(1 - 2.25577 * 10^{-5} * h)^{5.25588}\right)^{\frac{1}{3}}$$

Table 1 – Explanatory nomenclature table for Equation 1 and Equation 2

w_{site}	Calibrated nacelle speed
w_{std}	Measured nacelle wind speed
T_{site}	Nacelle ambient temperature (K)
T_{std}	15°C (288.15 K) ambient temperature
P_{site}	Air pressure at site
P_{std}	101325 Pa ambient air pressure
h	Site elevation in meters above sea level
$\boldsymbol{\rho_{std}}$	Calculated density at site
$\boldsymbol{\rho_{site}}$	1.225 kg/m^3 air density at sea level

To make the power curve calculations, the data is binned with the same range as the wind speeds. Only bins with at least 6 hours of data are used to get a representative result. Several calculations are made for the bins:

- Median output
- Standard deviation
- 10th percentile
- 90th percentile
- Power curve uncertainty i.e. standard deviation divided by power
- Sample count in the bin

3.3.2.2. Icing Events

Icing events are divided into three different classes by Task 19; a) decrease in production, b) standstill, c) overproduction due to the iced anemometer. Icing event class a) is started if the temperature is below 0°C, and power is below the 10th percentile of the reference power curve for 30-minutes or more. It ends if power is above the 10th percentile for 30 minutes or more.

For each 10-minute data point, it is decided whether that data point is classified as affected by ice or not. If the data point is classified as an iced-data point, and if nearby data points are also ice affected so that the data points create a 30-minute consecutive trace of ice-related data, then the data points are ice-losses.

Icing event class c) is started if the temperature is below 0°C AND power is above the 90th percentile of the reference power curve for 30-minutes or more. It ends if power is below the 90th percentile for 30 minutes or more. While icing event b) follows the same idea as icing event a) with a 10th percentile curve, the difference is that the icing event starts when the power is below 10th percentile AND results in a shutdown for at least 20 minutes. It ends if the turbine is started AND the power is above the 10th percentile for 30 minutes or more.

3.3.2.3. Production losses due to icing

Once the icing events have been identified the production losses can be calculated. The difference between the reference and actual measured output power for each time step is calculated.

3.3.3 *Kjeller Method*

Kjeller Vindteknikk is a consultancy company within the wind power and wind engineering industry in the Nordics. In their report, Hansson et al. (2016), together with Energiforsk, investigate six different methods, which are being analyzed. These methods can be divided into two different groups, where the first group is depending on one or more ice-free turbines on a wind power farm to be used as references. The other group which is preferred by Hansson et al. (2016), is based on wind and production data.

In the same report, a methodology for the post-construction of estimating production losses due to icing is presented. By adjusting varying densities according to IEC 61400-12-1 a taking the median wind speed bins at very 0.5 m/s just as others have (Byrkjedal et al., 2015; Davis et al., 2015; Homola et al., 2009; Task19, 2019) and filtering out the following data:

- Data with alarm codes and the time step after the alarm occurred.
- Data for periods with curtailed power output (i.e., periods when the wind turbine is operating in a lower capacity than it should).
- Data that may be affected by icing, temperatures below 3°C.
- Occasions when nacelle wind speed is more than two meters above cut-in, and the power production is less than 5 kW.

A reference power curve is then constructed by making a 10-percentile power curve for each turbine and not site-wise like Task19 (2019). This does also mean that Kjeller Vindteknikk did not take the overproduction due to iced anemometers into account is this paper, in contrast to Task 19, where a 90-percentile power curve is also used. Hansson et al., (2016), emphasize the need for a long-term reference dataset since there is a considerable variation in power output from one year to another. Furthermore, it is assumed that there is less icing on turbines at locations with low elevation and that it is more icing on turbines at high elevation locations, which are then validated in the report. Another distinctive difference is that Kjeller Vindteknikk filter away the nacelle wind speeds around the cut-in. Since the cut in is normally 4 m/s, all the data points with wind speeds below 6 m/s are not being accounted for by Kjeller in the reference curve.

The ice-losses are, however, defined almost identically to Task19 (2019). The 10^{th} percentile is used as a reference. All data points which are below this reference, have a temperature below 3° C, have a turbine which indicates normal operation, and that this happens three time steps in a row, are classified as ice losses.

3.4 De-icing systems

De-icing systems are a fairly new phenomenon in the wind power industry, and it was not until 2004 when the first de-icing systems were installed by Enercon (*The Ice Issue - The Ice Issue | Winterwind | Where Theory Meets Practice*, n.d.). De-icing systems depend greatly on measurements. Placed at the top of the wind turbine tower, the hub is located. Here, sensors are placed to check numerous weather data to operate the wind power plant and to maximize power production safely. When icing occurs, these sensors can be shut down or be unable to gather accurate information. This can cause misdirection of the rotor or that the steering of the plant stops operating event though the wind is within the legal speed limits (4-25m/s). Fakorede et al. (2016) wrote a comparison between ice protection systems where they concluded that improving the cold-climate performance of wind turbines has become a "sine qua non" condition, meaning it is a necessary action for the continued development of the wind power industry. While they state numerous de-icing systems, there are two that this literature study will focus on: Blade heating and OWI.

3.4.1 *Blade heating*

When discussing blade heating, there are generally two types of systems that are intended: Heated air and Electrically heated mats. These systems are implemented in the rotor blades. For Electrically heated mats, the system consists of heating coils or carbon fibers that are placed strategically on the blades, either inside the membrane or laminated on the surface of the blades. The coils are then heated by electricity taken from the grid at standstill; shown as negative power production in the SCADA data. The heated air technology is also used at a standstill; the concept is to inject warm air into the blades and warm the ice by heat flux. This system is used both for de-icing purposes but also for anti-icing, which prevent ice accretion.

Normally, one of these two systems are used but there are also examples when they have been used together. Wallenius & Lehtomäki (2016) write in their overview on cold climate wind energy challenges, that a combination of surface heating and hot air heating could lead to better coverage of ice protection in terms of efficiency over a wider area of ambient conditions.

For the blade heating to be turned on the sensors need to detect icing, normally, this is done by checking the reference power curve with the actual power production and the ambient temperature. If the sensors are detecting high wind, low temperature, and low power production (or in some cases: no production) the turbine is shut down. It is when the rotor is completely still that the heating is put on for a certain amount of time, then the ice is estimated to have time to slide off and the rotor is yet put in motion. If the power production is still low, the system is required to stop once again for another de-icing cycle. This procedure will continue until a production within proximity of the reference power curve is reached.

One reason for not operating with blade heating would be the risk for ice-throw. Ice from the rotor blades can be thrown 90 meters at a very high speed, which can cause a severe health and safety risk for the surrounding environment (Davis et al., 2015). The main reason for not running any kind of blade heating while running the turbine is however another. In 2011, Oliver Parent and Adrian Ilinca wrote a critical review on anti-icing and de-icing techniques for wind turbines. The reason that cooling of the blade from the slipstream would be so high that it would require extreme amounts of energy from the grid to heat the blade which would not make it beneficial to run the heating system

Blade heating can be both expensive and very power consuming. Since the blade heating requires the plant to stop the turbine, the possibility to produce power with slight ice-formation is completely removed, which means that we have a power loss higher than due to the actual icing. Yet, removing the ice makes further ice formation impossible, and the turbine will be able to operate without standing still.

3.4.2 *OWI – Operation with Ice*

OWI is a software for active pitch control. The system is not an ice protection technique, as Ville Lehtomäki mentions in his report for IEA in 2016, it is used for pitching the rotor blades in the optimal direction of the wind to keep the turbine operating throughout an icing event. When ice is formatted on rotor blades, the angle of attack is changed. What the OWI then does is that it uses the pitch system to find the optimal angle for maximum power production. It does not require additional power consumption and is easily installed in already erected pitch-regulated turbines.

Lehtomäki (2016) also mention that pitch systems can suffer when exposed to cold weather; insufficient lubrication of components can damage gears. When a turbine can no longer operate the pitch system, it will either have to wait until the ice melts, or it must rely on a blade heating system. Y. Zhang et al. (2020), therefore, propose a combination of electric heating and active pitch regulation to have a rapid and efficient de-icing.

3.5 Summary literature review

In Table 2, an overview is given for the different methodology approaches made by the earlier studies mentioned. Here, the most significant assumptions for this thesis are summarized.

Table 2 - Methodology assumptions

	Kjeller Vindteknikk : Hansson et al 2016	Byrkjedal et al 2016	Davis et al 2015	Aziz et al 2019	Homola et al 2009	Task 19
Is SCADA data used?	Yes	Yes	Uncertain	Yes	Uncertain	Yes
Is the data binned by 0.5 m/s?	Yes	Yes	Yes	Yes	Yes	Yes
Is the 90th percentile used as a reference?	No	No	No	No	No, 85th percentile	Yes
Is the 10th percentile used as a reference?	Yes	Yes	Yes	No	No, 15th percentile	Yes
Is the reference data filtered at +3° C and higher?	Yes	Yes	Yes	No	No, +2° C	Yes
Is the reference based on data for the entire site?	No	Uncertain	No	No	No	Yes
Does the reference data cover several years of data?	Yes	Yes	It should cover at least 1 year of data.	Yes	Yes	Uncertain
Is the ice data filtered at a nacelle temperature of +3° C and below?	Yes	Yes	Different scenarios, reaching from -2° C to +4° C	Uncertain	No, +2° C	Yes
Is iced data validated if it persists for at least 3 consecutive time steps?	Yes	Yes	Yes	No, two consecutive time steps	No	Yes
Is the data density corrected according to IEC 61400-12-1?	Yes	No	Yes	Yes	No	Yes

4 PROPOSED ICE DETERMINING METHOD

The assumptions made in the formation of this method hold its ground in the approaches made by the studies in the literature study. A combination of threshold power curve based on turbine operational status and measured temperature criterion was used to create the ice determining code. The code from which ice loss data will be extracted is made in R-studio with the datasets given by an SGRE server. Firstly, the code is downloading data by choosing the site, tower height, alarm codes, and the dates from the year to be analyzed. It is after the data-download that the data is processed.

From the literature study, it is concluded that the power curve should be based on the use of polynomial values to look at the linear regression. Further, the maximum theoretical power production is defined as the production of the turbine as if it was to operate with blades free from ice. The ice losses are calculated based on data for one site at a time. To ensure ice-free data, the reference power output data is based on data between the warmest months for Sweden, i.e., May throughout September. What alarm codes for which the central part of the filtrations was done on, is based on the combination of two recommendations made by other internal reports from SGRE, which has tried to make similar identifications of ice losses from SCADA data. Before any filtration is done on the raw data, NAN values are removed. Also, for both reference and ice datasets, the density is corrected by using the same calculation as Task19 (2019), stated in Equation 2 found in the literature study.

4.1 Site information

Two sites are initially investigated; they will be called Site 1 and Site 2. They are both located in the middle of Sweden. However, Site 2 is located higher up in the country compared to Site 1. Site 1 has 26 turbines installed with a tower height of 122.5m, whereas Site 2 has 48 turbines installed with a tower height of 115m. The turbines for both sites are of model SWT-113 from Siemens.

Site 1 has blade heating installed with electric heating mats on all turbines from the initial installation of the turbines. OWI was installed at Site 1 in the middle of December 2015 on 13 of the 26 turbines at the site. It was not until late November in 2017 that the remaining turbines were installed with OWI. A test was made on the site in the winter between 2017-2018, to investigate the performance of OWI, turbines with equal power production were identified and divided into pairs of two. These twin-turbines were then evaluated by running OWI on just one of them to compare the power production between an OWI turbine and a non-OWI turbine. Site 2 operates with OWI on all turbines; the installation of OWI was done in December 2016.

4.2 Reference Curve

The methods in the literature study suggest that a reference dataset should be used to form a reference curve. Therefore, a reference dataset is made where the 90th and the 10th percentile is used as threshold to identify iced affected data points. Percentiles are a robust metric and can be used to capture the variance of a variable, according to Davis et al. (2015). The 90th percentile is extracted to see if data points that are affected by an iced anemometer can be identified, yet these data points are not counted as ice losses. The curve itself, is based on data from four different years, site-wise, to eliminate fluctuations caused by elevation of different sites, precipitation and to ensure that the data is ice-free. The gradient and constant for each bin are used as a reference for the upper and lower threshold to identify the data points which are affected by ice.

From the literature study, it was unclear what kind of data was preferred to use for a reliable reference curve. While Hansson et al. (2016) use data for one turbine as reference and Task19 (2019) use data for an entire site, the amount of historical data that the reference is supposed to use is rather unclear, yet most of the literature suggests data from at least one year. In this thesis, the reference curve is based on 4 different years: 2016, 2017, 2018, and 2019. These years were chosen to smooth out the variation in power output from one year to another, which is emphasized by Hansson et al., (2016) in the literature study.

4.2.1 *Data pre-processing*

The data pre-processing is a crucial stage since filtering out data open the possibility that iced or non-iced data has been filtered out wrongly. The reference data is therefore filtered with five different filters to out rule iced data:

- Filter1: Filters out all data points that are below 3 degrees Celsius.
- Filter2: Filter based on data that have sufficient wind for production.
- Filter3: Filter away all data points which have a power output of 0 kW or below.
- Filter4: Filters out all alarm codes that have a power limit, which is not based on the nominal operation.
- Filter5: Filters out all alarm codes about actual turbine status, which can be related to icing.

4.2.2 *Threshold calculations*

In the linear equation, found in Equation 3 below, k is the gradient, and m is the constant for the slope of the line. Linear interpolation is used by both Task19 (2019) and Hansson et al. (2016). Both the gradient and the constant are calculated for the upper 90th percentile and the lower 10th percentile by binding the data into intervals of 0.5 m/s. The length between the minimum and the maximum velocity is therefore split by 0.5 to get the optimal number of bins. The gradient for each bin is then calculated with Equation 4, where y represents the measured power from the dataset, and x is the velocity given in the dataset. The m-constant could then easily be extracted with Equation 5.

Equation 3

$$y = k * x + m$$

Equation 4

$$k = \frac{y_{[i+1,1]} - y_{[i,1]}}{x_{[i+1,1]} - x_{[i+1,1]}}$$

Equation 5

$$m = y - k * x$$

4.3 Defining ice losses

4.3.1 *Scenarios*

A difference in temperature between the tip of the blade and nacelle is not uncommon. The distance from the tip of the rotor to nacelle is 56,5m for both Scenarios in this study; it is a parameter that needs to be taken into consideration. The temperature threshold used for the significant part (Byrkjedal et al., 2015; Hansson et al., 2016; Task19, 2019) of the studies in the literature study, is set to 3° C. However, there is no clear explanation to why this would be the optimal temperature.

Three scenarios are therefore analyzed to see how much-iced data is discovered when the temperature filter is changed from a temperature of 0 to 3 and 5 degrees Celsius. The scenarios are a type of sensitivity analysis but are referred to as “scenarios” to make it more distinguishable from the sensitivity analysis explained in the title further down, which is not as extensive as the scenarios.

4.3.2 *Data pre-processing*

The dataset will cover at least 6x24x365 data points since the data is in a 10min resolution. Which equals to 52 560 data points for each turbine. As mentioned earlier, the data needs to be downloaded. To get the relevant data, 46 different variables where downloaded, leaving each site-dataset to be at least a 46x 52 560*turbines matrix. To minimize the number of data points, the dataset is filtered early in the code. Instead of filtering out the data points which can be connected to ice, which is done in the reference curve, these are the points that should be highlighted and saved in the new, minimized, dataset.

- Filter 1: Filter the operational status of the turbine and takes away the turbine stoppage not related to icing. Such as the untwisting of cables or wind speeds that are too high.
- Filter 2: Filters out all alarm codes that have a power limit which is not based on the nominal operation.
- Filter 3: Filter based on data that have sufficient wind for production.
- Filter 4: Filters out all alarm codes about actual turbine status which cannot be related to icing.

When downloading the data, the variables must be chosen beforehand. Date, time, velocity, power output, temperature, and alarm code are therefore extracted. The alarm codes are many and are divided into different categories. The categories concerned are stated below:

Description of alarm category	Filtered on
Turbine operational state	Stops which can be caused by icing
Source of active power limit	Limits defined by Nominal and Converter power
Newest turbine alarm code	Icing events and normal production.
Actual turbine status	Sufficient wind for production

These alarms have multiple codes for various occasions, and one year of data can have hundreds of different codes. To make the process of finding the relevant alarm codes more efficient the data is filtered based on codes that are only connected to icing events and normal production by looking at the newest turbine alarm code.

4.3.3 *Calculating ice losses*

Data points found below the 10th percentile threshold that also have a temperature below 0 degrees for Scenario 1, 3 for Scenario 2 or below 5 degrees for Scenario 3, and have a turbine that is operating normally is not enough to count as a data point affected by ice. If the mentioned requirements are met and they are found for no less than 3 consecutive time steps, that is when the data point is defined as affected by ice.

In the code, the reference gradient and the slope constant are together with the measured velocity used to calculate the expected power output for every data point in every bin. In this part of the code, all NAN values are removed so that every single data point that has gone through the data pre-processing and is checked against the calculated expected power value. This is a very time-consuming step in the code and the most important part. The measured data point which is then highlighted as smaller than the calculated expected power, is then saved as data affected by ice.

The icing events are then found and can be extracted. The ice losses are calculated by using the difference between the expected power and the actual measured power. Since the data is given as kW for 10 minutes, the data was converted to kWh by dividing the power output with 6. Thereafter the code summarized the data for each turbine and year. Further processing of the data was made in Excel to convert the annual ice losses to both MWh and in percentage for an entire site.

4.4 Correlation factors

Since temperature and precipitation have a big impact on ice build-up, it is interesting to see whether any correlation can be found between the annual ice losses, temperature, and precipitation. January, February, and December are what SMHI defines as winter months, which is why the average temperatures and precipitation given in the tables below are based on the monthly average precipitation for these months. The SMHI data was given by the metrological station closest to the site location and were extracted from SMHI – Swedish Meteorological and Hydrological Institute (2020). Only data for the investigated years were extracted.

Table 3 - Average winter temperature and precipitation Site 1.

Year	Monthly (Dec/Jan/ Feb) average temperature [°C]	Monthly (Dec/Jan/ Feb) average precipitation [mm]
2016	-7.93	23.07
2017	-7.30	27.13
2018	-9.37	43.80
2019	-6.10	30.77

Table 4 - Average winter temperature and precipitation Site 2.

Year	Monthly (Dec/Jan/ Feb) average temperature [°C]	Monthly (Dec/Jan/ Feb) average precipitation [mm]
2016	-7.77	39.13
2017	-5.93	44.20
2018	-8.53	39.50
2019	-6.77	34.77

The reason for this data being extracted from SMHI is that precipitation is not something that can be found in SCADA. Precipitation measurements are made by additional software that is not connected to SCADA, and since the data is not measured in the same time resolution as SCADA it was not investigated whether it could be possible to merge these two data sets.

4.5 Sensitivity Analysis

To validate the assumptions made for the ice loss determining method, a sensitivity analysis has been performed.

4.5.1 *Reference curve*

A sensitivity analysis is made for the power reference curve. The raw data for the power reference curve was changed from May-Sep to Jan-Dec, and June-July to see how much-iced data could be explained by adding more/fewer data points. Hence it was only analyzed for 2019 on Site 1 on Scenario 2, where the temperature threshold was set to 3° C.

4.5.2 *Temperature threshold*

A minor sensitivity analysis was also made on the temperature thresholds beyond the ones in Scenario 1, 2, and 3. In this analysis, a threshold was set to 1.5 and 6 degrees respectively to see how much more/fewer ice losses that could be found. It was however conducted for data from the year of 2019 on Site 1, with a reference curve based on data from May to September (the same reference curve as for the scenarios).

5 RESULTS

The ice losses found in Table 5, Table 8 and Table 9 will be presented with a manipulation-factor to normalize the values. Therefore, the actual ice losses, which are first calculated in percentage of the expected power output, is divided with a number. This number will be unknown to the reader yet known by the author of this report and SGRE. The normalized ice losses are then multiplied with 100. This normalization is further explained by Equation 6. Both sites are divided by the same number so that it is possible to show a ratio between the two different sites.

Equation 6

$$Normalized\ ice\ losses = \frac{Actual\ annual\ ice\ losses}{m_{factor}} * 100$$

This is done to avoid exploiting confidential data from the owner of the wind farms. Additionally, it is important to highlight the fact that the power curves in the sections below have thousands of data points. And that what may seem like one data point might have hundreds or thousands more that are on top of each other, or very close to one another.

5.1 Reference curve

In Figure 4 and Figure 5, the reference power curves for the two sites are presented. These reference curves are used in Scenario 1, 2, and 3. The reference curves are based on data between May-Sep in the years of 2016-2019. The blue line represents the 10th percentile while the 90th percentile is represented by the red line. The pink points in the actual power curves below represent the reference curve data. A distinctive dip can be seen in the 10th percentile line for Site 2. Both reference curves have a 10th percentile and a 90th percentile line which seamlessly merge at the highest bins. The reference curve for Site 1 has undeniably several data points near a zero power production at higher wind speeds above 10 m/s than the reference curve for Site 2 shows.

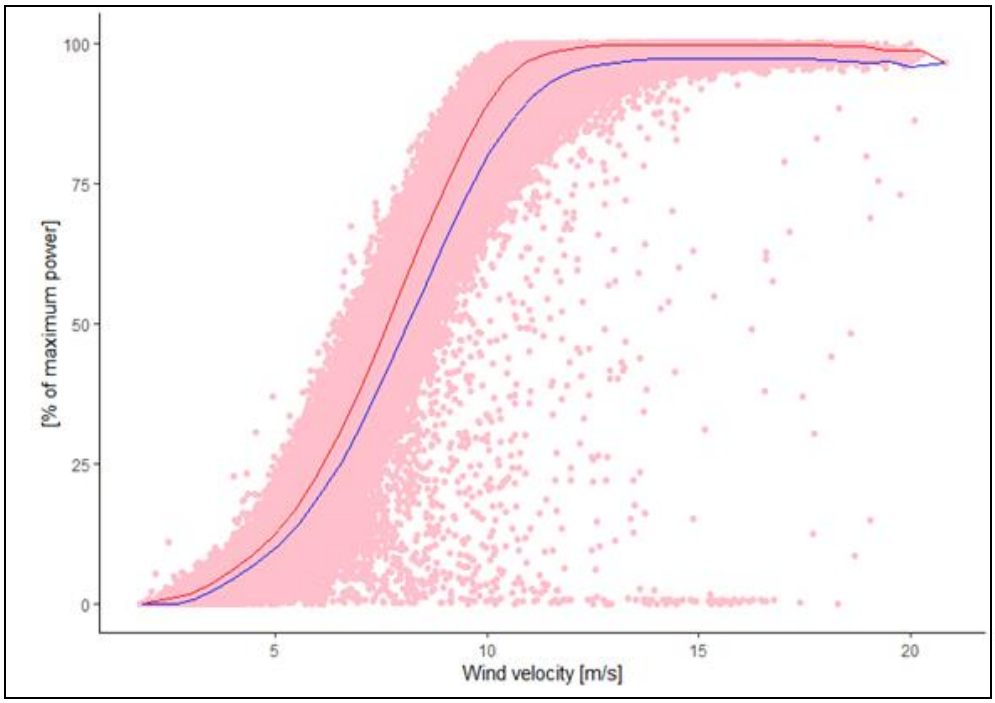

Figure 4 - Reference curve for Site 1. The y-axis is showing the percentage of the maximum nominal power and the x-axis showing the wind velocity in m/s.

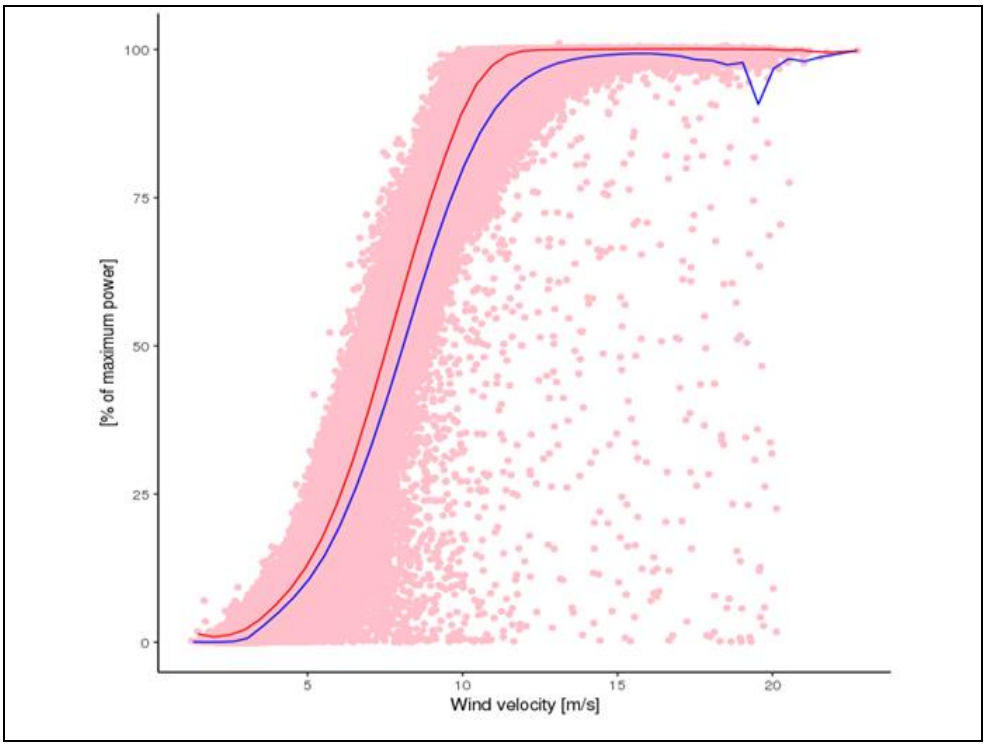

Figure 5 - Reference curve for Site 2. The y-axis is showing the percentage of the maximum nominal power and the x-axis showing the wind velocity in m/s.

5.2 Actual power curve

The colored diagrams that are featured in the sections below are the actual power curves of the sites, presenting the turbine power data and the nacelle wind speeds. The blue line represents the 10th percentile, while the 90th percentile is represented by the red line. The pink points in the actual power curves below represent the reference curve data. The purple points are the raw data for the specific year, whereas the yellow points are the data points that are affected by ice. The points below the 10th percentile is therefore defined as ice losses while the yellow points above the 90th percentile are the data points that are affected by an iced anemometer.

5.2.1 *Scenario 1*

In Scenario 1, a temperature threshold of 0° C is set to identify ice losses. As can be seen in Figure 6 and Figure 7, the actual power curves are departing from the reference curves. Site 1 is diverging more distinctively than Site 2. In Figure 6, the power curves for 2016, 2017, and 2019 show a clear deviation from the reference curve. This type of deviation can also be detected in 2016 for Site 2, although not as definite as for Site 1. The ice losses for 2018 in Figure 6 are more concentrated near a zero power output.

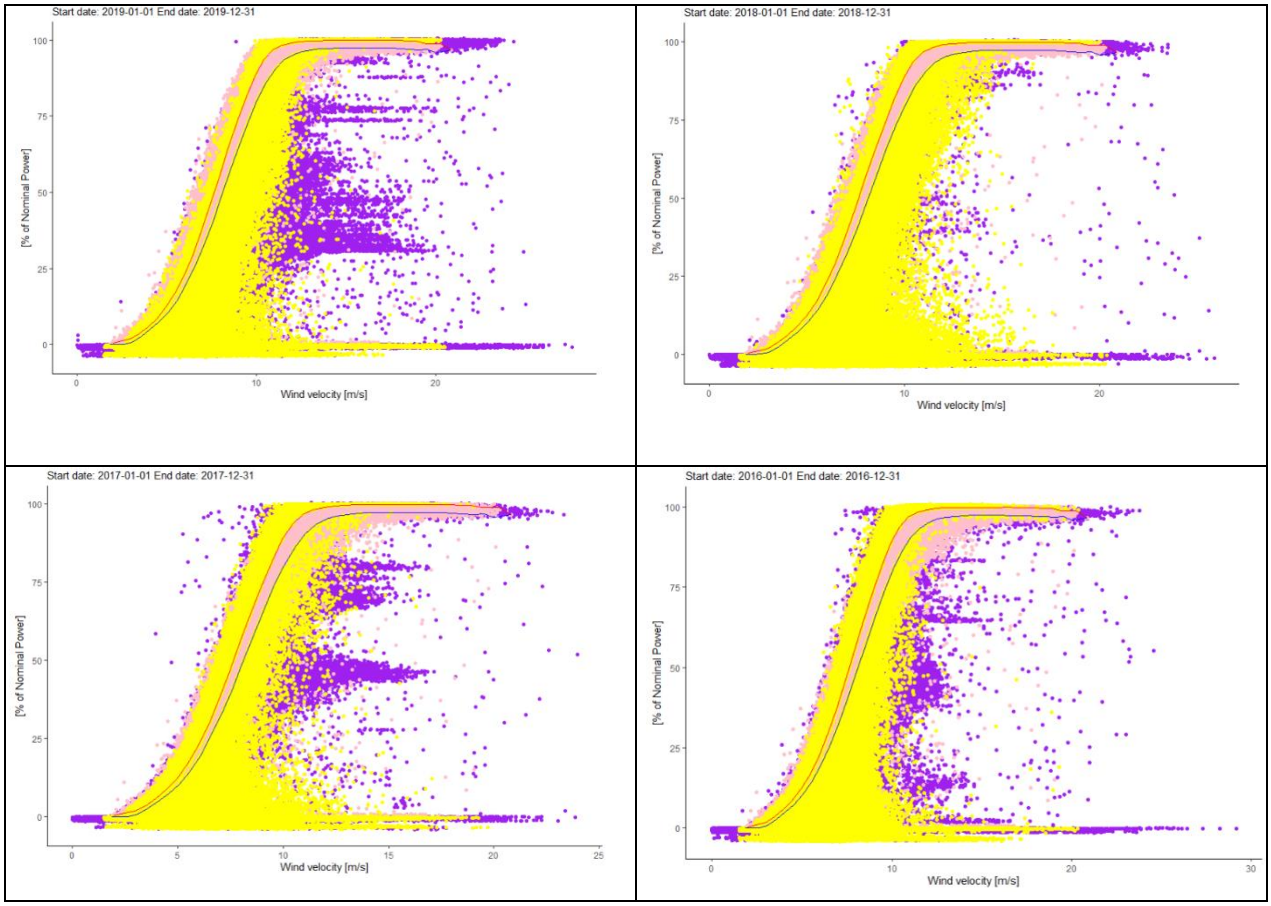

Figure 6 - Actual power curve for Site 1. Scenario 1. From the upper left corner to the right are the years: 2019 and 2018. To the lower-left corner to the right are the years: 2017 and 2016.

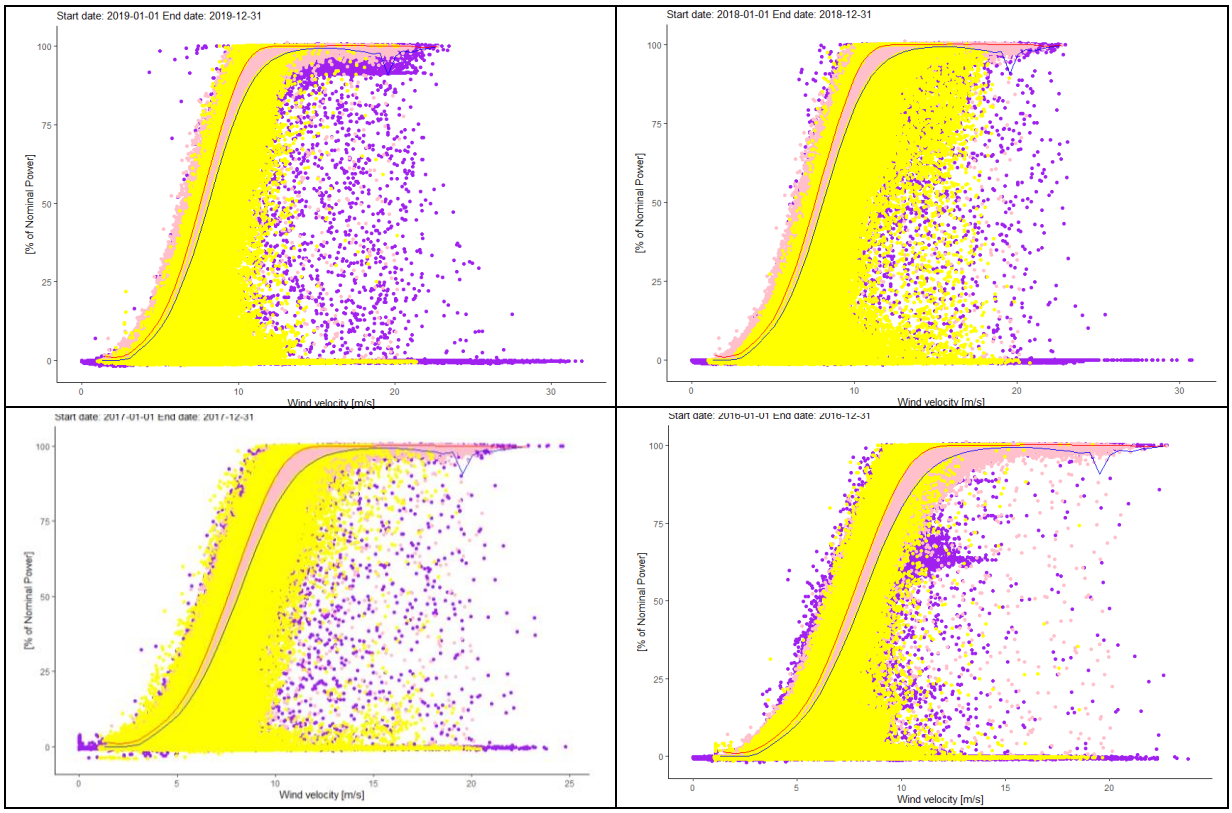

Figure 7 - Actual power curve for Site 2. Scenario 1. From the upper left corner to the right are the years: 2019 and 2018. To the lower-left corner to the right are the years: 2017 and 2016.

5.2.2 *Scenario 2*

Scenario 2 uses a temperature threshold of 3° C to identify ice losses. In Table 5, the ice losses for the turbines for Site 1, which underwent the test between December 2017 and February 2018, are presented. As can be seen, the ice losses where in general higher in 2018 than in 2017, but the difference between the turbines installed with OWI and the turbines without is much bigger for 2018 than for 2017.

Table 5 - Annual ice losses Site 1, Scenario 2, turbines with OWI vs. turbines with no OWI.

	Average ice loss with manipulation factor- 2018	Average ice loss with manipulation factor - 2017
Turbines with OWI	155%	120%
Turbines without OWI	182%	119%

As can be seen in Figure 8, the actual power curves for Site 1 are presented. There is a lot of the raw data that does not follow the characteristics of the reference curve, especially for 2019. The raw data, contain higher wind speeds than the wind speeds found in the reference curve. This can be seen for all the years since the percentile curves reach an end around 20 m/s, whereas the plot over 2016 clearly shows that there are velocities measured at a much higher speed.

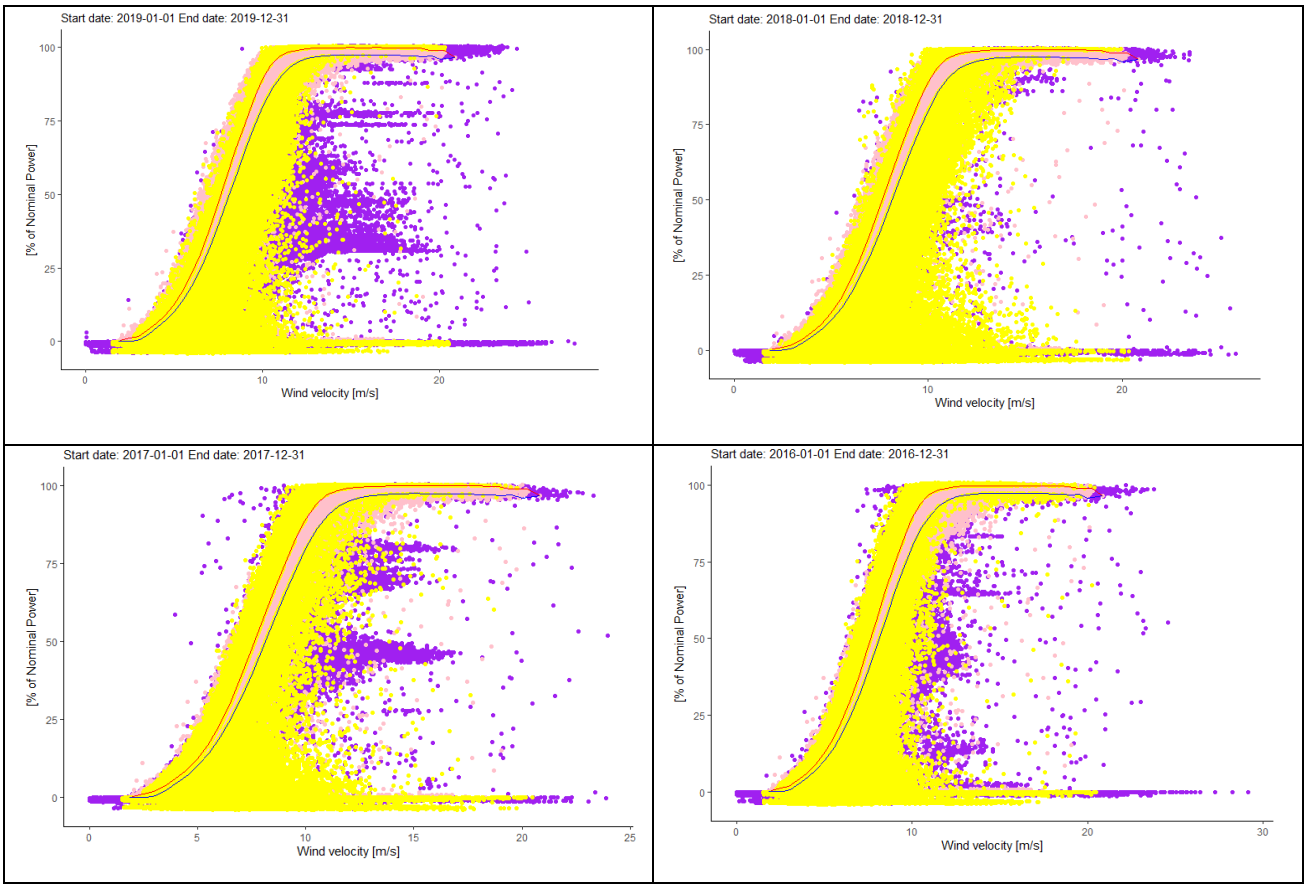

Figure 8 – Actual power curve for Site 1. Scenario 2. From the upper left corner to the right are the years: 2019 and 2018. To the lower-left corner to the right are the years: 2017 and 2016.

In Figure 9, the actual power curve for Site 2 in Scenario 2 is presented. In the bottom left corner, the plot for 2018 is showing a lot of data points defined as ice losses.

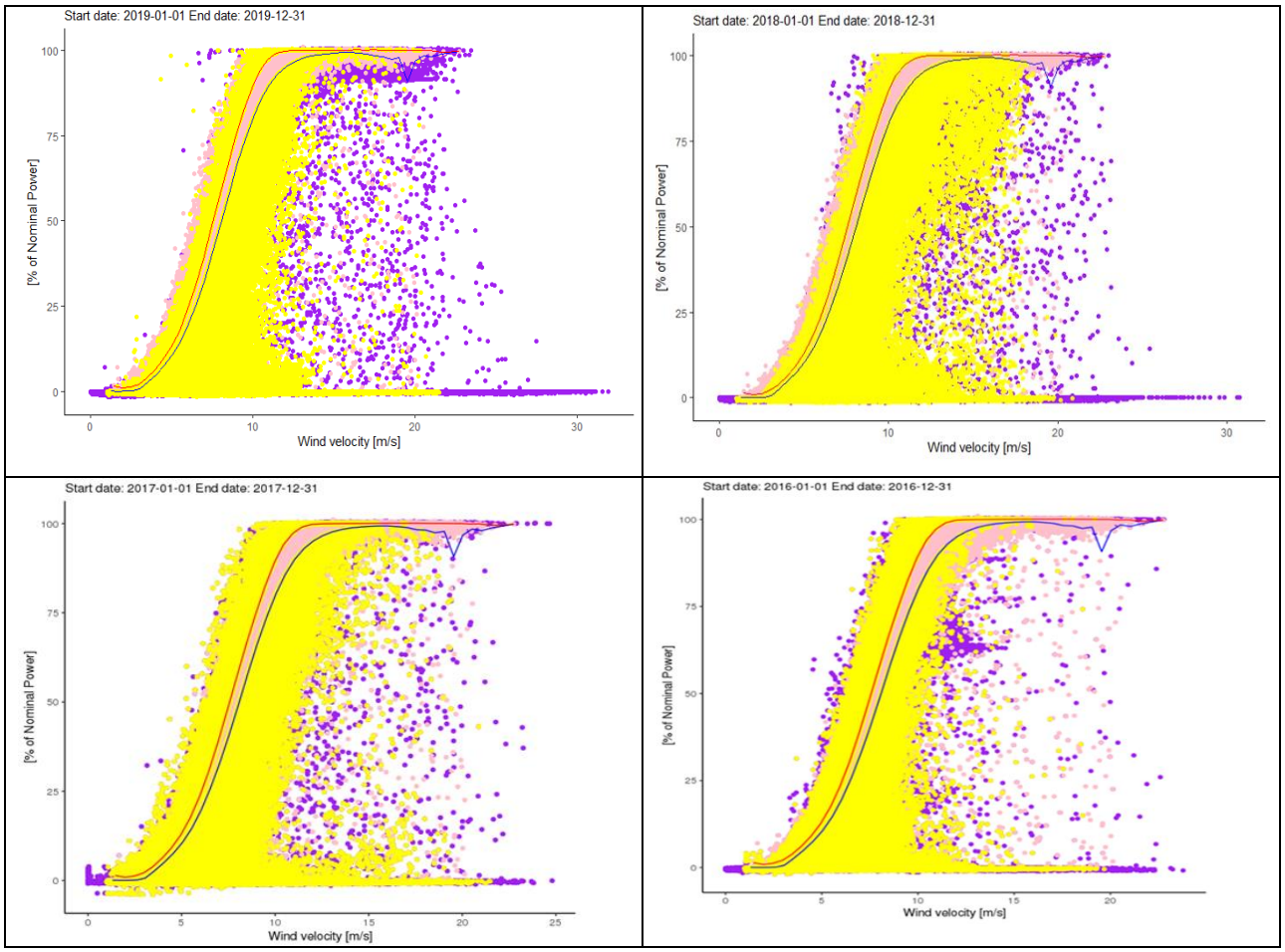

Figure 9 - Actual power curve for Site 2. Scenario 2. From the upper left corner to the right are the years: 2019 and 2018. To the lower-left corner to the right are the years: 2017 and 2016.

5.2.3 *Scenario 3*

In Scenario 3, a temperature threshold of 5° C is set to identify the ice losses. More data points are identified here to be ice losses compared to the other two Scenarios, as suspected. This is further presented in section 5.4. More of the data points above the 90th percentile is also found to be affected by ice for both Site 1 and 2. Otherwise, the actual power curves do not differ significantly from the other two scenarios, neither for Site 1 nor for Site 2.

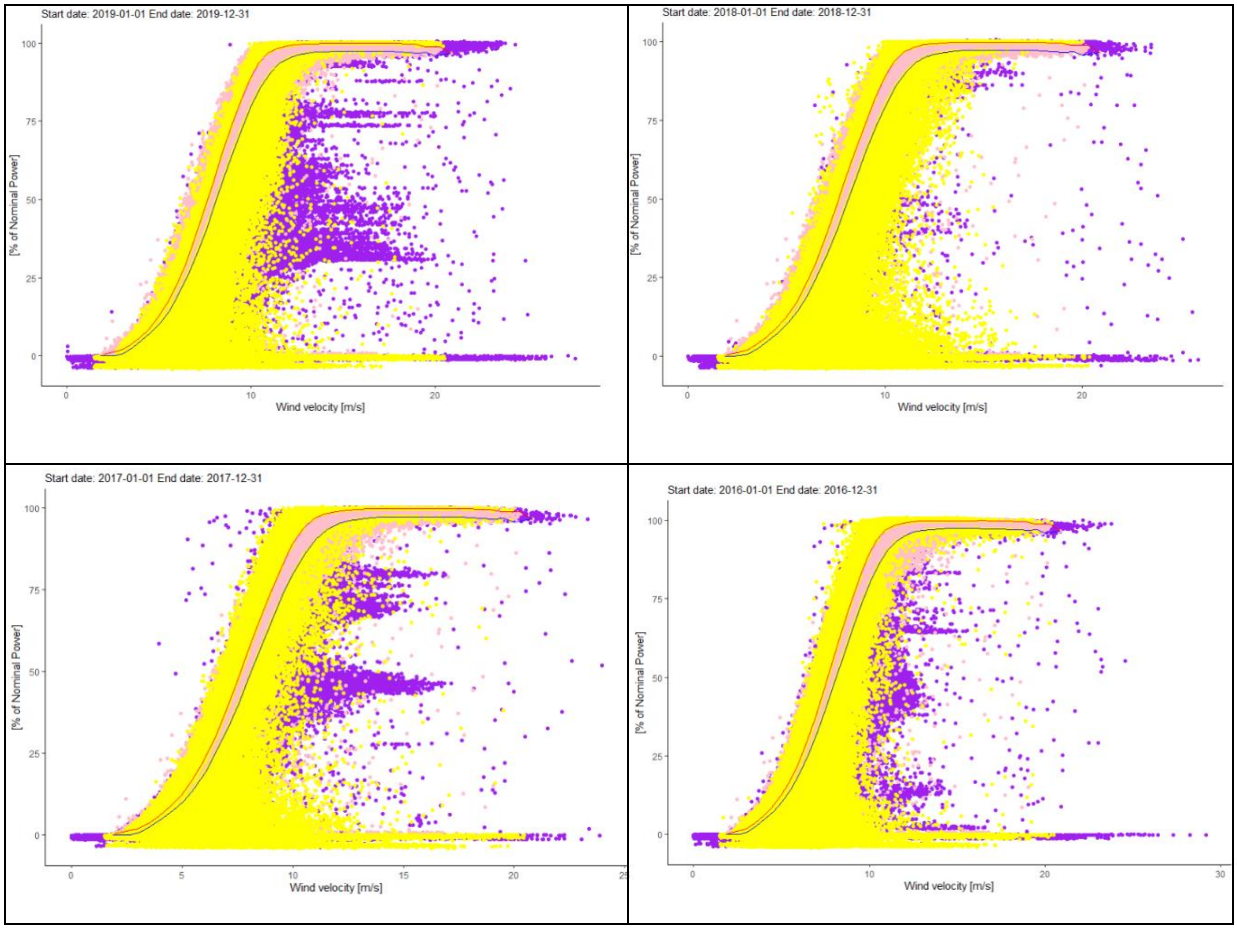

Figure 10 - Actual power curve for Site 1. Scenario 3. From the upper left corner to the right are the years: 2019 and 2018. To the lower-left corner to the right are the years: 2017 and 2016.

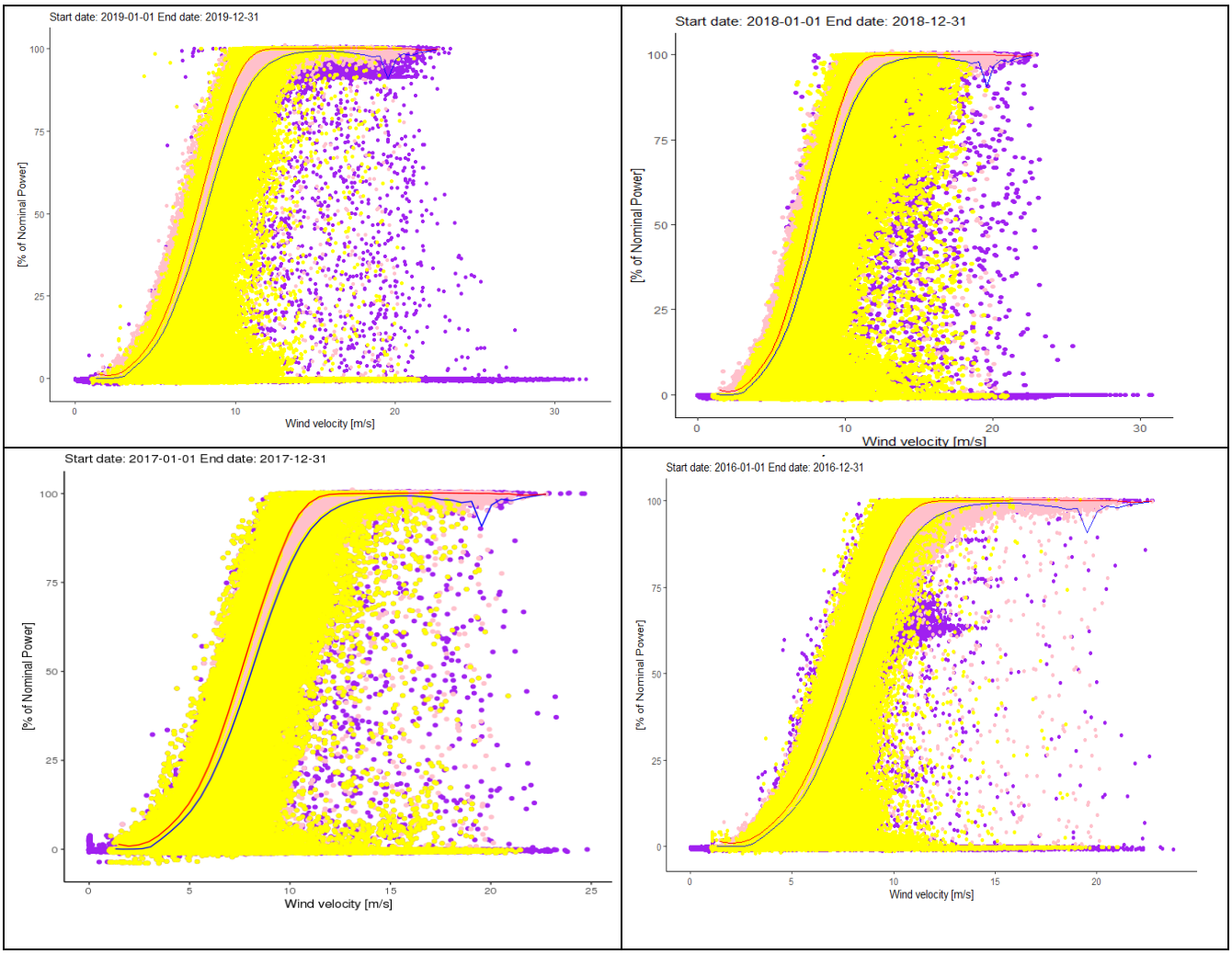

Figure 11 - Actual power curve for Site 2. Scenario 3. From the upper left corner to the right are the years: 2019 and 2018. To the lower-left corner to the right are the years: 2017 and 2016.

5.3 Alarm codes

The alarm codes which were filtered out from the raw data are presented in Table 6 and Table 7. Before the first alarm filter, the raw data has, besides a density correction, not been tampered with. After the three first alarm filters, there are only data points where the turbine is operating normally, have enough wind for production and turbine stops related to icing. It is at the last filter where all alarm codes which cannot be related to icing is removed, leaving the raw data to be ready for binning.

Table 6 - Table over the number of unique alarms existing in the processed data after the different filtrations for Site 1.

Year	Before 1st Alarm filter	After 3rd Alarm filter	After last Alarm filter
2016	204	196	189
2017	208	201	193
2018	194	188	182
2019	226	222	211

Table 7 - Table over the number of unique alarms existing in the processed data after the different filtrations for Site 2.

Year	Before 1st Alarm filter	After 3rd Alarm filter	After last Alarm filter
2016	222	207	206
2017	223	218	213
2018	245	240	229
2019	245	234	227

5.4 Ice-losses

Table 8 shows the normalized annual ice-losses for all scenarios for Site 1. The ice losses are divided with a number and then multiplied with 100 to avoid exploiting confidential data from SGRE; this number is referred to as "manipulation factor" in Table 8 and Table 9. By only looking at Scenario 1, it seems as though 2017 is the year with the least amount of identified ice losses, and 2018 is the year with most ice losses. The column to the far right presents the percentual increase of identified ice losses between Scenario 2 and 3. These two are especially interesting to look at since the literature claim that the threshold should be set to 3° C. As can be seen, the percentile increase of identified ice losses was 6 % when the threshold was moved from 3° C to 5° C.

Table 8 – Site 1: Normalized annual ice-losses for all scenarios.

Site 1	**Annual ice losses with manipulation factor %**	**Annual ice losses with manipulation factor %**	**Annual ice losses with manipulation factor %**	**Percentual increase of identified ice losses between Scenario 2 and Scenario 3**
Year	Scenario 1 - 0° C	Scenario 2 - 3° C	Scenario 3 - 5° C	
2016	108%	123%	131%	5,64%
2017	105%	119%	123%	3,17%
2018	162%	168%	172%	2,28%
2019	113%	133%	141%	5,59%

It can be seen in Table 9 that 2017 was the year with the least amount of identified ice-losses and that 2016 was the year with most identified ice losses.

Table 9 - Site 2: Normalized annual ice-losses for all scenarios.

Site 2	**Annual ice losses with manipulation factor %**	**Annual ice losses with manipulation factor %**	**Annual ice losses with manipulation factor %**	**Percentual increase of identified ice losses between Scenario 2 and Scenario 3**
Year	Scenario 1 - 0° C	Scenario 2 - 3° C	Scenario 3 - 5° C	
2016	165%	186%	191%	2,91%
2017	98%	114%	121%	6,04%
2018	126%	140%	151%	7,15%
2019	121%	140%	146%	4,04%

5.5 Sensitivity Analysis

Two sensitivity analyses were done; Table 10 presents the results given by adding two scenarios for Site 1. The temperature threshold is tested for 1.5° C and 6°C. The data itself is only from the year of 2019 and the reference curve used is the same as for the other scenarios earlier presented for Site 1.

Table 10 - Site 1, 2019: Normalized ice losses for new temperature thresholds 1.5° C and 6° C.

	1.5° C	6° C
May-Sep	126%	144%

The second sensitivity analysis is based on data from Site 1 in 2019. Here, the same three temperature threshold mentioned earlier in the Scenarios section was used. Hence the reference data is changed. The Jan-Dec scenario shown in Table 11 is showing a higher detection of ice losses than the May-Sep scenario. The June-July scenario shown in the same table is showing a lower detection of ice losses than the May-Sep scenario for the 5° C threshold.

Table 11 - Site 1, 2019: Normalized ice losses with reference curves with data from Jan-Dec and June-July.

	Annual ice losses with manipulation factor %	Annual ice losses with manipulation factor %	Annual ice losses with manipulation factor %
Scenario	0 ° C	3° C	5° C
Jan-Dec	115%	135%	143%
May-Sep	113%	133%	141%
June-July	113%	133%	140%

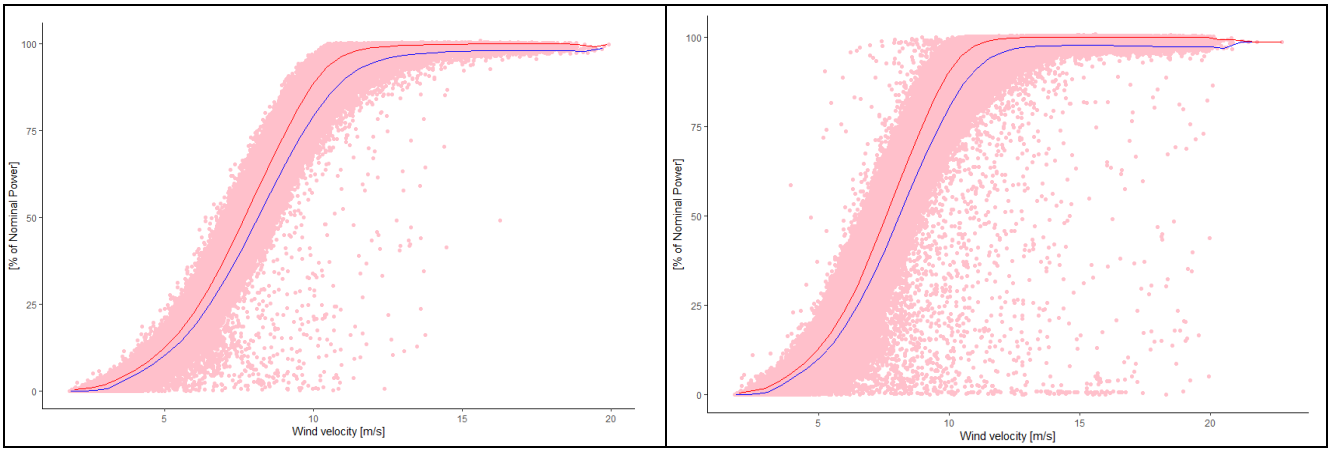

Figure 12 - Reference curve for Site 1 with reference data. From the left to the right: Scenario June-July and Scenario Jan-Dec.

6 DISCUSSION

The complexity of defining ice losses is founded in the variability of the variables and the variables that are considered. This will change the result, depending on the assumptions taken. In the first section below, the data filtration will be discussed and evaluated. The ice losses, defined by the code, are being analyzed in section 2. Furthermore, the sensitivity analysis will validate the results in the third section.

6.1 Data pre-processing

As can be seen in Table 6, 15 unique alarm codes are filtered out for Site 1 in 2016, 2017, and 2019. The exception is 2018, which filtered out 12 alarm codes. What is interesting to see here is how much the filters influence the raw data and how great importance each filter has. That the same number of unique alarm codes are filtered out in 2016, 2017, and 2019 is more of a coincidence rather than the rule. By comparing Site 2, more variant numbers of unique alarm codes are filtered away. As an example, the year of 2016 and 2018 filters out 16 alarm codes, as 2017 filter 10, and 2019 removed 18 codes. The exception for Site 1 was the lower filtration in 2018, which could be explained by the test that was conducted at the site in January and February that year. What is also interesting is that the last filter, which removes all alarm codes that are not connected to iced data, only filtered out one alarm for Site 2 in 2016. Since OWI was not installed in the park until late November 2016, the last filter might only be connected to alarm codes related to the OWI system, which makes the filter irrelevant for turbines operating without OWI.

The reference power curve for Site 1 is based on data from May throughout September to out rule the possibility of iced data, yet it is shown in Figure 4 that there are multiple outliers in the data despite the filtration made. In the filtration, alarm codes related to iced data were removed. It was found, by visual inspection of the actual power curves in Figure 6, Figure 8, and Figure 10, that the outliers in the reference curve were not considered to be iced data points by the ice detection code. The filtration for the reference curve was done in a way that the reference curve would be left with a few iced affected data points as possible without having to investigate all the alarm codes and data points one by one. Investigating the alarm codes and data points individually would be a very inefficient way of filtering the data since there are thousands of data points to go through. This makes the filtration vulnerable, yet since the filtration is based on previous studies made internally by SGRE, it should be enough of filtration to validate that the outliers are not affected by ice.

As mentioned in section 4.3.2, the dataset which is used in this thesis is very big. The reference data is built upon millions of data points, and the benefit with a dataset with so many data points is that the given result have variations and is therefore capable of presenting the reality in a nuanced and credible way. The disadvantage with big dataset is that few have access to it. Though SCADA data is used widely by the industry, it is hard to get a hold of such big dataset unless given by the industry which limit the research. This makes the work of standardizing an ice detection method much more difficult. A big dataset with

millions of data points take time to process, it is therefore important to point out that the amount of data limited this thesis to only look at two different sites. By optimizing the code further, the code could run faster, and more sites could be investigated. Note that the speed of the code will always be limited by the computer's processor and frame memory.

The reference power curve for Site 2 has a dip in the 10th percentile threshold at 20 m/s, generally, there are very few data points at higher velocities. This makes the 10th percentile curve a bit doubtful to use at cut-out speeds since the data is affected more heavily by outliers which are not completely filtered out, as clearly presented in Figure 4. The last bins in both reference curves have the 90th and 10th percentile curves merging into the same curve. Just as the case for Site 1, it is impossible to find ice losses by checking the expected power against the measured power since there is no reference gradient nor reference slope to calculate the expected power. To dodge the uncertainty of a percentile bin with few data points, a solution could be to set a threshold for a minimum number of hours of data in a bin. This was done by Task19 (2019), and the minimum threshold was set to 6 hours of data. However, the 6-hour threshold needs to be investigated further to see how much the outliers influence the percentiles, and if 6 hours is enough.

6.2 Ice losses

The ice losses shown in Table 8 have been normalized. The ice-losses without the manipulation factor ranges from 5 to 10 percent of the annual expected energy output which is lower than the 10-35% as suggested by Hansson et al. (2016b) and Yirtici et al. (2019b). However, it should be noted that the sites investigated are both installed with software's to minimize the ice losses. Still, the ice losses are up to 10% of the annual expected energy output. Leaving them well in between the range suggested in the literature study.

By looking at the ice losses in Table 8, it is shown that 2016 was the year with the second-lowest ice losses for Site 1, Scenario 1. In contrast, it was the year with the highest percentual increase of identified ice losses between Scenario 2 and Scenario 3 compared to the other years. In Table 3, the average winter temperature for 2016 is -7.9° C, which seems like a normal average temperature, compared to the other years investigated which range from -6.1 to -9.4° C. Between the years of 2016 and 2019 the precipitation is caught in a range from 23.1 to 43.8mm, which is quite the range, compared to Site 2 which ranges from 34.8 to 44.2mm in the years from 2016 to 2019. Comparing the ice losses, 2016 has the second-lowest ice losses for Site 1 with 123% for Scenario 2, with 2017 being the lowest year with a 119% ice loss with the manipulation factor. The year 2017 had an average winter temperature of -7.3° C, which is warmer than for 2016, yet the precipitation is higher at 27.13mm for 2017. The percentual increase of identified ice losses shown in Table 8 is lower for 2017 than for 2016, which could be related to the higher annual winter temperature for 2017.

It was found that with a 40% higher annual ice loss ratio than 2017, the ice losses for 2018 was the highest ice losses for Site 1 between the four years that were investigated. While 2018 was the year with the highest ice losses, it was the year with the lowest average temperature, the highest precipitation, and had the lowest percentual increase of identified ice losses between Scenario 1 and Scenario 2. It can be concluded by comparing the ice losses in Table 8 and Table 9 with the temperatures and precipitations in Table 3 and Table 4 that the precipitation has a high impact on the ice losses.

By looking at the precipitation and the temperature data from SMHI, it can be seen that this specific year had an extremely high precipitation, which makes the formation of ice more likely to happen. Thus, most of the ice losses were found at the 0° C temperature threshold, which could be correlated back to a low average temperature, meaning it was a rather cold winter. Not to mention, the data for December 2017 and January to February 2018 should be taken cautiously since the test with OWI was performed during this time. As the OWI system is not running, the de-icing is. The heating mats are turned on when there is enough ice formed on the blades that it cannot operate further until the ice is melted enough to operate at nominal power, the turbine will be at a standstill. This ice formation and ice-build happen at lower temperatures, which is a reason why most ice losses are identified at lower temperatures.

It is known from the site owner of Site 2 that the park was affected heavily by ice in December 2019. For Site 1, 2019 was also the second most ice affected year. However, it can be concluded that it was not, in fact, an unusually icy year for Site 2 since a comparison between the data for 2017 and 2018 show that the ice losses for 2019 were between those two years. 2016 should not be compared to the other years since the OWI system was installed in December 2016, yet what is interesting is that 2016 has 60% higher ice losses compared to 2017 which had the lowest annual ice losses for the years investigated. Showing the great ability of the OWI system for Site 2.

The difference between turbines with OWI installed and turbines without can be seen by viewing the actual power curves for Site 1 under section 5.2. Here, the turbine is operating with OWI in 2016, 2017, and 2019 which will cause a shift in the maximum power output in the actual power curve. This happens because the turbine is settling at a power output below the nominal power instead of shutting down immediately so that the heating mats can be turned on. As shown by Hansson et al. (2016) in Figure 5-12, this happens to the power curves when turbines use similar software as the OWI from SGRE. What can be seen in figures Figure 6 to Figure 11 is that these data points are entirely filtered away. This can have an amendment to the ice loss results. It can be discussed if this data should be filtered away or not, since these data points are affected by ice and would have produced a zero power output if the software was not installed. It is altogether clear that Site 1 would have had higher ice losses if all turbines were disconnected to the OWI software during the test.

Even though Site 2 had both an overall precipitation and ice loss which were higher than for Site 1, it should be recognized that Site 1 run with both OWI and heating mats. A comparison between the two sites is tough to do by looking at the ice losses solely since de-icing systems are installed and re-installed, which will have a big impact on the ice losses. However, the temperature and precipitation together with the ice losses are interesting to compare to one another. In each scenario, the same pattern is repeating itself, as the temperature threshold is moved to a higher temperature, more ice losses are found. This shows that a temperature threshold at 3° C might not be high enough to find all ice losses, as implied in the literature study.

6.3 Data accuracy and correlation

Briefly mentioned in section 3.2.2, the correction factor for the wind speed anemometers which are occasionally changed, has not been considered while calculating the losses. Since the data is checked for several different years, it is hard to identify how much this correction factor is affecting the calculated ice losses. Considering that the reference power curve is also based on data from several different years with the aim to smooth out such kinds of disparity, it is an error that should not cause any bigger miscalculations. As can be seen in Figure 6 to Figure 11, the actual power curves for each scenario, for both sites show a major impact on the iced anemometers. Many data points are found to be overshooting the 90th percentile curve which is a measurement uncertainty claiming that the energy is higher at lower velocities. When in the reality, the wind velocity is measured wrongly by either ice affected measurement instruments, or because of the placement of the anemometers, which are usually positioned behind the rotor.

Since the expected power for each year is calculated based on the velocity bins given by the raw dataset for that year, the data points over the 90th percentile has an impact on the expected power. By calculating the expected power without these overshooting data points, a lower expected power should be anticipated. Yet the 10th percentile curve would also be shifted, making it a zero-sum game for the ice losses calculated in percentage of annual energy output. Now, if the ice losses are calculated in kW, the figures might not reflect the entire truth if the data points overshooting the 90th percentile are not to be considered. To know how these faulty measurements should be quantified, a further study needs to be done to see how this affects the accuracy of the ice detection.

The correlations found between ice loss, precipitation and weather could be further investigated by using Principal Component Analysis, Neural Network or implement other correlation methods such as Deep learning. This could also be performed on the data points to find ice losses to strengthen the data accuracy and remove the uncertainties which comes with threshold settlements used in this thesis.

6.4 Sensitivity analysis

6.4.1 *Reference curve*

A sensitivity analysis was made to see if the outliers in the reference curve for Site 1 could be filtered out by delimiting the reference data to June and July. It was then discovered that even though much of the outliers where removed, the wind speeds were too low compared to the raw data. Meaning that raw data with wind speeds over 19m/s cause the code to be unable to find the expected power because there is no reference gradient nor constant for the velocity bins at those wind speeds. Bins where raw data exist but a reference gradient and slope cannot calculate a reference power output, whereas a threshold to find the ice losses becomes impossible - making the code unable to identify possible ice losses for higher velocities. This could be explained by the fact that higher velocities are reached in the winter months, and since the reference data is between June and July, the wind never reaches a higher speed.

The reference power curve was therefore extended to capture data from May to September. When the site power curve for Site 1 was made in the original scenarios, it was clear that the data points with higher velocities, over 21 m/s, where not found in the reference data. Therefore, a second sensitivity analysis was conducted where the reference power curve data was extended from May-Sep to include all months for a year, namely the months from January to December. Despite this, it was shown that the Dec-Jan curve, which was only done for Site 1, could not explain higher velocities than the May-Sep data. The reference curve for Jan-Dec had also a merge in the 90th and the 10th percentile curves as the reference curve for May-Sep did, and the merging happened at the same velocity for both reference curves due to few data points in the bin. This is not uncommon, since the velocities as rarely over 19m/s in Sweden, even during winter.

The outliers found in the Jan-Dec reference data were also many more than the outliers in the May-Sep data, implying that the code was unable to filtrate all the outliers. Since this causes the 90th and 10th percentile thresholds to be shifted, and an extended interval between the percentiles includes more data points, which results in an expected increase of annual ice losses. The results in Table 11 show that there was a 0,6 percent rise of annual ice losses when the Jan-Dec months were compared to the May-Sep reference curve, a rather insignificant increase. Yet seen to power output, the ice losses are much higher for Jan-Dec than for the two other scenarios. Moreover, since the reference curve is between the same wind speed interval, this rise in ice losses must be due to the influence of the outliers. However, the change is so small, it could be negligible.

6.4.2 *Temperature threshold*

As both Table 8 and Table 9 shows, ice losses can be found when the temperature is over 3° C, a minor sensitivity analysis was made when this threshold was moved to 1.5° C and 6° C to see how the code behaves and to see if more ice losses could be found over 5° C. Task19 (2019) and Davis et al. (2015) both mention a bias of +2° C to +3° C in the nacelle temperature. If a bias of 3° C were to be considered, then ice losses at 3° C would, in fact, be converted to ice losses at 0° C. Leaving all measured temperatures above 3° C to be three degrees less than they should. Ice losses above 0° C would then be due to ice which was created at a lower temperature but has yet to melt away. As can be seen in Table 8 and Table 9 the percentual increase of defined ice losses between Scenario 2 and Scenario 3 are in general lower for Site 1 which have de-icing installed, compared to Site 2 which only operates with OWI, giving space for further ice accretion and standstill.

Since ice is formatting at temperatures of 0° C and the bias is 3° C one could argue that the threshold should be set to 3° C. Hence, as can be seen in Scenario 3, ice losses can be identified at +5° C. Davis et al. (2015) found ice losses at temperatures higher than +4° C. A minor analysis on Site 1, when the temperature threshold was set to +6° C, gave higher ice losses. This is probably one of the biggest source of error in this report, as it certainly is for anyone studying ice losses.

7 CONCLUSIONS

From the literature study conducted, it was concluded that ice losses are generally defined at a temperature threshold at +3° C. Yet, a lack of motivation for this led this thesis to test three different temperature threshold scenarios. The threshold which was suggested by the literature was found to be unsatisfactory and the temperature threshold suggested in this thesis should be extended to at least +5° C, as ice losses were identified at +6° C. Instrumental icing, the phenomenon where ice remains at a structure and/or an instrument is concluded to be the reason for how ice losses still occur at +6° C.

The only conclusion to draw from the filtering of alarm codes is that the ice-related filter is only needed if OWE is installed since the alarm codes for iced data only exist then. Which might make it harder to have an ice-free reference data in a park without OWI, since the filter cannot be applied to the reference data to remove iced data points. Furthermore, the expected power and the ice loss results are affected by the change of correction factor, but since the data is checked for several different years, it is an acceptable margin of error that cannot be quantified.

A 10^{th} percentile threshold is used to find the ice losses and 3 consecutive time steps to out rule defect data. How extensive the data for a reference curve should be was uncertain in the literature, still, several sources claim that a reference curve should consist of at least one-year worth of data. This thesis, therefore, used a raw data set covering four years of data from May through September to smooth out the variations that occur from year to year due to weather fluctuations. A sensitivity analysis showed that using reference data for May to September brought enough data to cover the velocity bins at higher wind speed bins. A reference data for all the yearly season should therefore not be needed.

By following the presented method given in this thesis, the ice losses are determined and analyzed in a robust and simple way. Leading to a determination of ice losses, which are in the scope and aim of this study. Therefore, it can be concluded that ice losses can be identified by analyzing historical SCADA data. Both sites investigated are installed with systems which purpose is to minimize the ice losses, yet the identified ice losses are normally not negligible and are typically around 5-10% per year for both sites. The actual power curves show that the code can identify ice losses, even for sites operating with de-icing systems.

So, as the literature study suggests, the ice losses would be larger if no de-icing systems where of use, how much more substantial these ice losses would be are in need to be further investigated. Also, the study should be extended to look at more wind farms to validate these claims. Further, it can be concluded that precipitation correlates strongly to ice losses and that low temperature and high precipitation is the best conditions for ice formation as high temperature and low precipitation is the worst conditions.

8 SUGGESTIONS FOR FURTHER WORK

This thesis is just a springboard for the development of this ice determining code. In the future work, the code itself could be developed to run faster and to be more user friendly. The sensitivity analysis should be extended to investigate the data points above the 90th percentile, the work should be focusing on quantifying these faulty measurements and their impact on the ice loss results. A further inspection of which alarm codes should be removed from the raw data and the reference data could be made to delimit the outliers. Also, the outliers themselves should also be investigated further to validate that they are for sure not connected to iced data. To use Principal Component Analysis, Deep learning or Neural Network might enhance the ice loss accuracy and remove the uncertainties with filtering of data, percentiles and temperature thresholds.

Investigating whether to set a threshold for the limited amount of data to dodge the uncertainties that comes with bins with too little data could also be of interest. And investigating if 6 hours of data is enough data to represent a bin. The conclusions drawn in this thesis about de-icing systems and comparisons against sites without de-icing systems could be further validated by investigating more sites. By looking at more sites the understanding for when ice losses occur and how different de-icing systems impact the annual ice losses could strengthen the incentives for implementing de-icing systems and software's like OWI.

REFERENCES

Aziz, U., Charbonnier, S., Berenguer, C., Lebranchu, A., & Prevost, F. (2019). SCADA data based realistic simulation framework to evaluate environmental impact on performance of wind turbine condition monitoring systems. *2019 4th Conference on Control and Fault Tolerant Systems (SysTol)*, 360–365. https://doi.org/10.1109/SYSTOL.2019.8864769

Byrkjedal, Ø., Hansson, J., & As, K. V. (2015). *Development of operational forecasting for icing and wind power at cold climate sites*. 4.

Davis, N. N. (2014). *Icing Impacts on Wind Energy Production*. 157.

Davis, N. N., Byrkjedal, Ø., Hahmann, A. N., Clausen, N.-E., & Žagar, M. (2015). Ice detection on wind turbines using the observed power curve. *Wind Energy*, *19*(6), 999–1010. https://doi.org/10.1002/we.1878

Fakorede, O., Feger, Z., Ibrahim, H., Ilinca, A., Perron, J., & Masson, C. (2016). Ice protection systems for wind turbines in cold climate: Characteristics, comparisons and analysis. *Renewable and Sustainable Energy Reviews*, *65*, 662–675. https://doi.org/10.1016/j.rser.2016.06.080

Gonzalez, E., Stephen, B., Infield, D., & Melero, J. J. (2019). Using high-frequency SCADA data for wind turbine performance monitoring: A sensitivity study. *Renewable Energy*, *131*, 841–853. https://doi.org/10.1016/j.renene.2018.07.068

Hansson, J., Lindwall, J., & Øyvind, B. (2016). *Quantification of icing losses in wind farms*. https://energiforskmedia.blob.core.windows.net/media/21259/quantification-of-icing-losses-in-wind-farms-energiforskrapport-2016-299.pdf

Homola, M. C., Ronsten, G., Nicklasson, P. J., Langesgt, L., & Ab, W. (2009). *Energy production losses due to iced blades and instruments at Nygårdsfjell, Sveg and Aapua*. 5.

IEAWind-Task19. (2019). [Python]. IEA Wind Task 19. https://github.com/IEAWind-Task19/T19IceLossMethod (Original work published 2019)

IRENA. (2019a). *Future of wind: Deployment, investment, technology, grid integration and socio-economic aspects (A Global Energy Transformation paper)*.

IRENA. (2019b). *Global Energy Transformation: A Roadmap to 2050 (2019 Edition)*. 52.

IRENA. (2020). *Innovative solutions for 100% renewable power in Sweden*. 116.

Kåberger, T. (2020, February 7). *A decade of expansion ahead*. Winter Wind 2020, Åre, Sweden.

Laakso, T., Baring-Gould, I., Durstewitz, M., Horbaty, R., Lacroix, A., Peltola, E., Ronsten, G., Tallhaug, L., & Wallenius, T. (2010). *State-of-the-art of wind energy in cold climates*. 74.

Laakso, T., Talhaug, L., Ronsten, G., Cattin, R., Baring-Gould, I., Lacroix, A., Peltola, E., Wallenius, T., & Durstewitz, M. (2009). *Wind Energy in Cold Climates IEA Task 19 – Outlook 2010*. 5.

Lehtomäki, V. (2016). *Wind Energy in Cold Climates Available Technologies—Report*. 120.

Letcher, T. M. (Ed.). (2017). *Wind energy engineering: A handbook for onshore and offshore wind turbines*. Academic Press, an imprint of Elsevier.

Marti, I. (2017). *2 2017 IEA WIND TCP ANNUAL REPORT*. 164.

Papatheou, E., Dervilis, N., Maguire, A. E., Campos, C., Antoniadou, I., & Worden, K. (2017). Performance monitoring of a wind turbine using extreme function theory. *Renewable Energy*, *113*, 1490–1502. https://doi.org/10.1016/j.renene.2017.07.013

Parent, O., & Ilinca, A. (2011). Anti-icing and de-icing techniques for wind turbines: Critical review. *Cold Regions Science and Technology*, *65*(1), 88–96. https://doi.org/10.1016/j.coldregions.2010.01.005

Reuters. (2016). *Siemens, Gamesa to form world's largest wind farm business—Reuters*. Siemens, Gamesa to Form World's Largest Wind Farm Business - Reuters. https://www.reuters.com/article/us-gamesa-m-a-siemens/siemens-gamesa-to-form-worlds-largest-wind-farm-business-idUSKCN0Z22JC

Sathyajith, M. (2006). *Wind Energy: Fundamentals, Resource Analysis and Economics*. Springer-Verlag. https://doi.org/10.1007/3-540-30906-3

Skrimpas, G. A., Kleani, K., Mijatovic, N., Sweeney, C. W., Jensen, B. B., & Holboell, J. (2016). Detection of icing on wind turbine blades by means of vibration and power curve analysis: Icing detection in wind turbines. *Wind Energy*, *19*(10), 1819–1832. https://doi.org/10.1002/we.1952

SMHI. (2020, February 28). *Årsmedeltemperatur*. Klimatindikator - Temperatur. https://www.smhi.se/klimat/klimatet-da-och-nu/klimatindikatorer/klimatindikator-temperatur-1.2430

Sohoni, V., Gupta, S. C., & Nema, R. K. (2016). A Critical Review on Wind Turbine Power Curve Modelling Techniques and Their Applications in Wind Based Energy Systems. *Journal of Energy*, *2016*, 1–18. https://doi.org/10.1155/2016/8519785

St. Martin, C. M., Lundquist, J. K., Clifton, A. (ORCID:0000000196985083), Poulos, G. S., & Schreck, S. J. (2016). Wind turbine power production and annual energy production depend on atmospheric stability and turbulence. *Wind Energy Science (Online)*, *1*(2), Article NREL/JA-5D00-66360. https://doi.org/10.5194/wes-1-221-2016

Stoyanov, D. B., Sarlak, H., & Nixon, J. D. (2020). Operational Strategies for a Large-Scale Horizontal-Axis Wind Turbine During Icing Conditions. In A. Sayigh (Ed.), *Renewable Energy and Sustainable Buildings* (pp. 839–846). Springer International Publishing. https://doi.org/10.1007/978-3-030-18488-9_69

The Ice Issue—The Ice Issue | Winterwind | Where theory meets practice. (n.d.). Retrieved April 20, 2020, from https://winterwind.se/the-ice-issue/

van der Linden, S. L., Leiserowitz, A. A., Feinberg, G. D., & Maibach, E. W. (2015). The Scientific Consensus on Climate Change as a Gateway Belief: Experimental Evidence. *PLOS ONE*, *10*(2), e0118489. https://doi.org/10.1371/journal.pone.0118489

Wallenius, T., & Lehtomäki, V. (2016). Overview of cold climate wind energy: Challenges, solutions, and future needs. *WIREs Energy and Environment*, *5*(2), 128–135. https://doi.org/10.1002/wene.170

Wizelius, T. (2015). *Vindkraft i teori och praktik*. Studentlitteratur.

Yirtici, O., Ozgen, S., & Tuncer, I. H. (2019). Predictions of ice formations on wind turbine blades and power production losses due to icing. *Wind Energy*, we.2333. https://doi.org/10.1002/we.2333

Zhang, L., Liu, K., Wang, Y., & Omariba, Z. (2018). Ice Detection Model of Wind Turbine Blades Based on Random Forest Classifier. *Energies*, *11*(10), 2548. https://doi.org/10.3390/en11102548

Zhang, Y., Chen, L., & Liu, H. (2020). Study on ice adhesion of composite anti-/deicing component under heating condition. *Advanced Composites Letters*, *29*, 2633366X2091244. https://doi.org/10.1177/2633366X20912440

MÄLARDALEN UNIVERSITY
SWEDEN

P.O. Box 883, SE-721 23 Västerås, Sweden **Phone: +46 21 101 300**
P.O. Box 325, SE-631 05 Eskilstuna, Sweden **Phone: +46 16 153 600**
E-mail: info@mdh.se **Webb:** www.mdh.se